MGH/MIT/HMS Athinoula A. Martinos Center
for Biomedical Imaging

Multimodal EEG/fMRI Imaging for Neuroscientists

Giorgio Bonmassar, Ph.D.

Cognitive 2015
Nice, March 2015

Non-invasive Brain Functional Imaging Methods

Method	Physical Principle
Positron Emission Tomography (PET)	Emission/Detection of Positrons
Single-Photon Emission Computed Tomography (SPECT)	Emission/Detection of Gamma Rays
Magnetic Resonance Imaging (MRI)	Nuclear Magnetic Resonance (NMR)
Electroencephalography (EEG)	Electrical Potentials
Magnetoencephalography (MEG)	Magnetic Fields
Electrical Impedance Tomography (EIT)	Changes in Tissue Complex Dielectric Constant
Optical Imaging (NIRS)	Light Absorption/Scattering
Transcranial Doppler Sonography (TCD)	Ultrasound Doppler Effect

Space Vs. Time

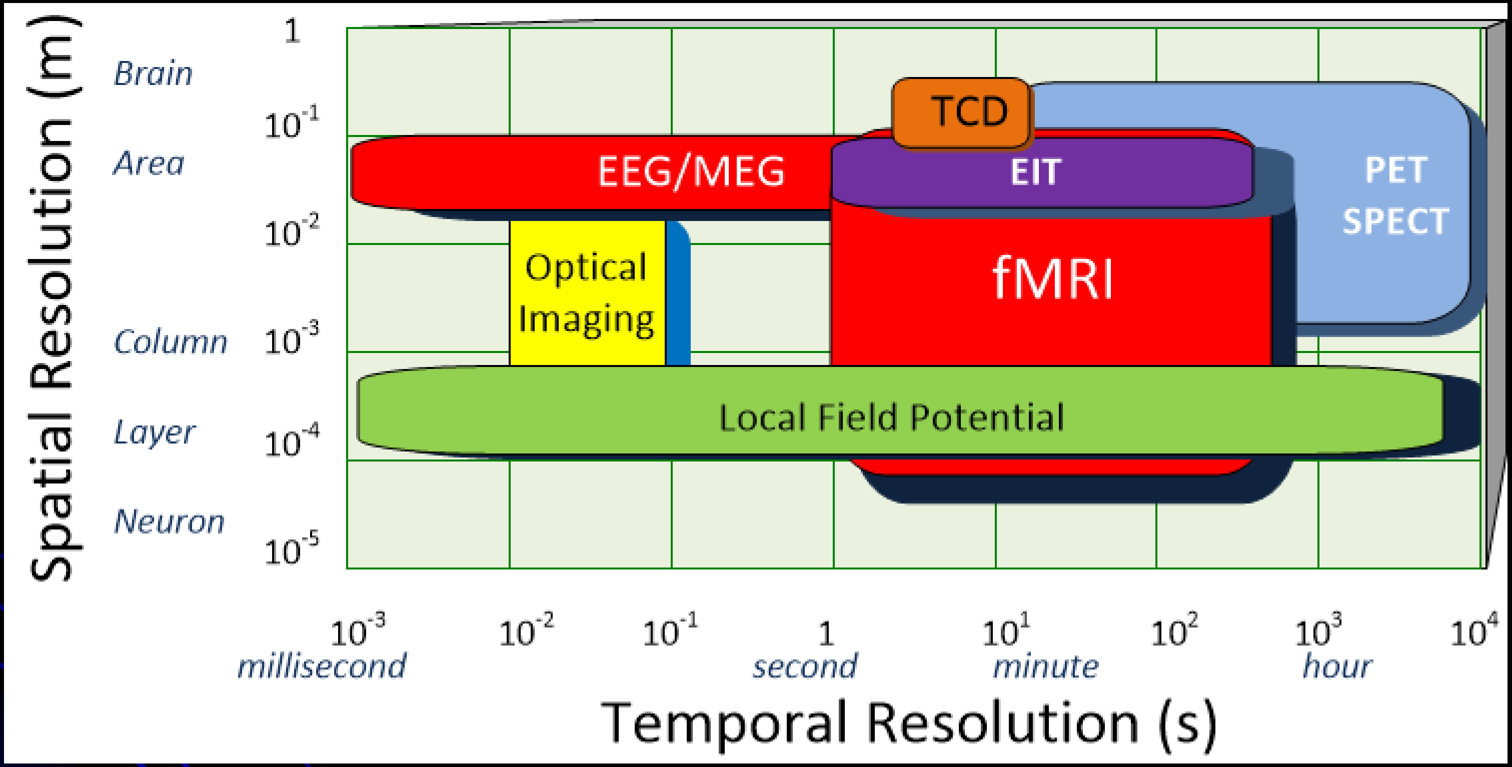

Post-synaptic Extra-Cellular Potentials

Excitatory (EPSP)

Inhibitory (IPSP)

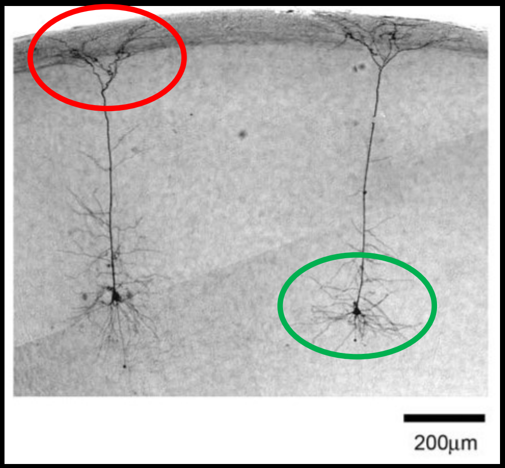

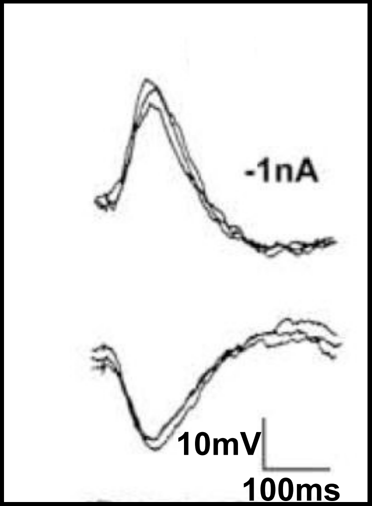

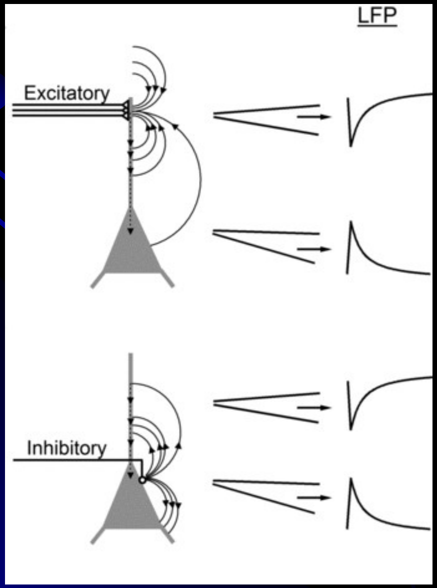

Synaptic input generates current sinks and sources along dendritic axis (Oren 2010 J.Physiol.)

PSP vs. EEG signals

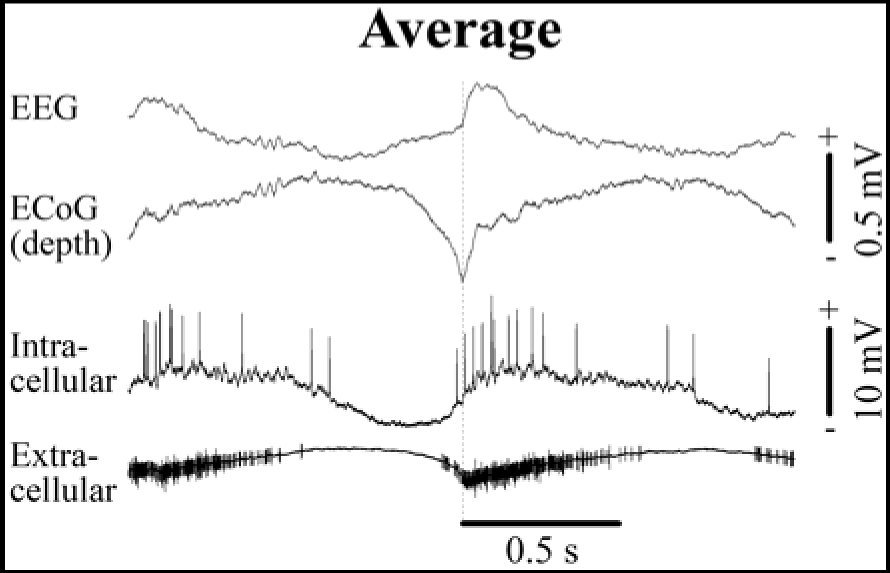

Amizica, Science 2010

Missing Sources:

Likelihood of PSP to be visible in the EEG depends on:

- Population size/type (e.g., cortex patch size/stellate cells)
- Synchronicity (e.g., null phase)
- Depth (e.g. brain stem evoked potentials)
- Orientation (e.g. radial)
- Cancellation/shielding (e.g., two opposite sulcus dipoles/thalamic)
- SNR issues (e.g., statistical processing)

PSP vs. fMRI signals

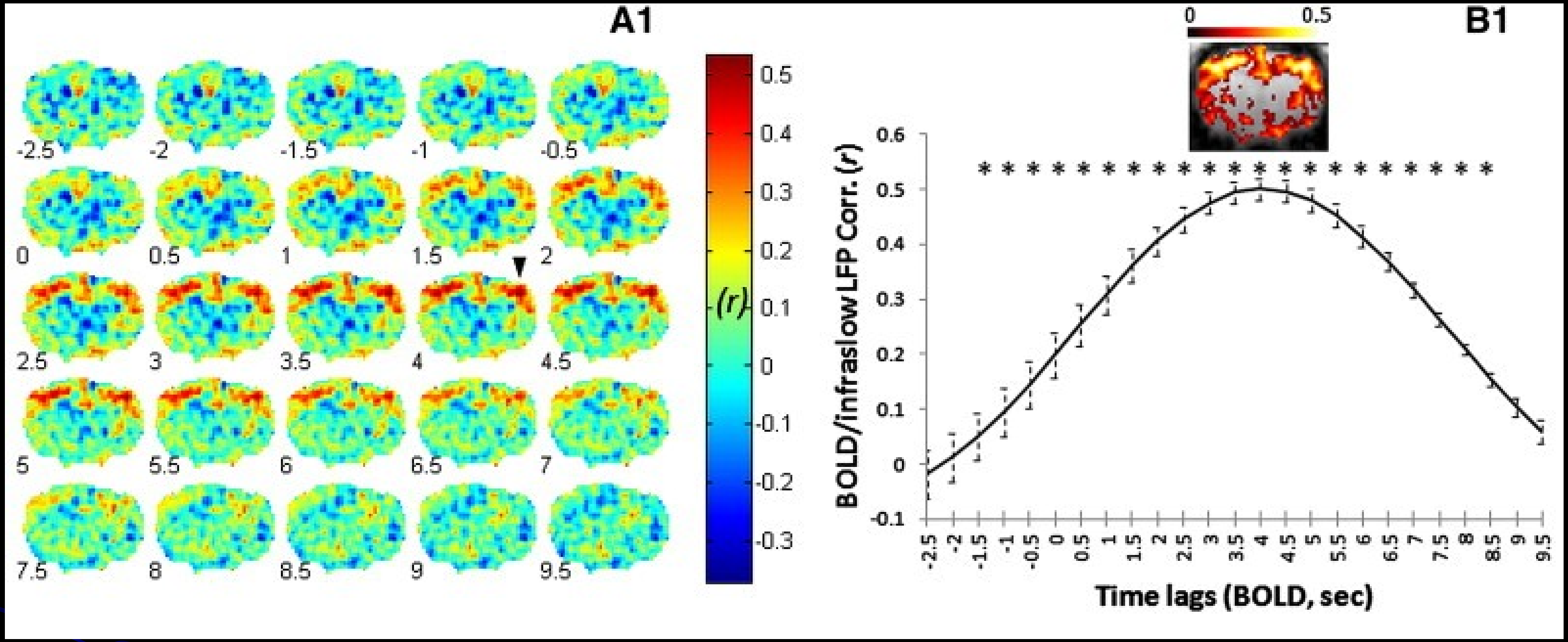

Pan, Neuroimage 2013

Missing Sources:

Likelihood of EPSP to be visible in the fMRI depends on:

- SNR issues (e.g., statistical processing)
- Presence of artifacts (e.g., temporal areas)
- Paradigm/Sequence (e.g. auditory studies)
- Random events in time (e.g., epileptic interictal spikes)
- BOLD washout/CO_2 (e.g., hypercpania)
- Small modification of cortical metabolic consumption

What are the advantages of EEG/fMRI?

- ✓ High spatial (MRI – mm and sub mm resolution) and temporal (EEG - ms resolution).
- ✓ Better chances to capture intrinsic brain states using multimodality (missing sources).
- ✓ Allow to study brain network connections by combining sophisticated electrical source imaging and causal dynamic analysis.
- ✓ Allow for studying BOLD synchronized neuronal firing, such as high frequency gamma oscillations.

Why Concurrent EEG/fMRI?

- Clinical
  - ✓ Epilepsy.
  - ✓ Intraoperative imaging (e.g., BIS).

- Neurophysiology
  - ✓ Sleep fMRI Studies (e.g., NREM studies)
  - ✓ Anesthesia and other drug research (e.g., Halothane’s sites of action)
  - ✓ Neuro vascular coupling between hemodynamic and electrodynamic .
  - ✓ Data Fusion: high temporal resolution of EEG with high spatial resolution of fMRI

Concurrent ERP/fMRI vs. recording separately

- ✓ Identical sensory stimulation, neurophysiologic events, subjective and behavioral experience (replicating the setup inside/outside the MRI can be very challenging).
- ✓ Long-term priming or learning (e.g., direction of motion – any limited number of novel stimuli).
- ✓ Monitoring ERPs as a prior for fMRI statistical analysis (e.g., VEPs and during migraine attack).
- ✓ Scanner noise (EPI) or MRI environment can influence the timing and amplitude of ERPs (auditory and auditory/visual).

Advantages of Ultra High MRI

- High-spatial resolution and high signal-to-noise ratio (SNR) BOLD signal (Gati et al. 1997; Van der Zwaag et al. 2009; Yacoub et al. 2001)
- Magnetic Resonance Spectroscopy (MRS):
  1. energy metabolism like glucose and creatine.
  2. neurotransmitters like glutamate and gamma-aminobutyric acid (GABA).
  3. compounds involved in cell growth like choline or in axon growth like N-acetylaspartate.
  4. compounds involved in osmoregulation like taurine and inositol.
  5. molecules that are antioxidants, like glutathione and vitamin C.

Outline

1. Devices & MRI Safety
   - ✓ No additional risks to the subjects
   - ✓ No effect on the quality of the diagnostic information
2. fMRI Image quality
3. EEG Signal Quality
   - ✓ Kalman filtering
4. Experimental Data
5. Electrocorticogram (ECoG)

1. SAR Recommendations

- The United States Food and Drug Administration (USFDA) limits the exposure to RF energy SAR < 3.2 W/kg (Head)

$$SAR = \frac{\sigma_c}{2\rho}\left|\vec{E}\right|^2$$

- Any pulse sequence must not raise the temperature by more than 1° Celsius

Human Head Models for EM forward solution

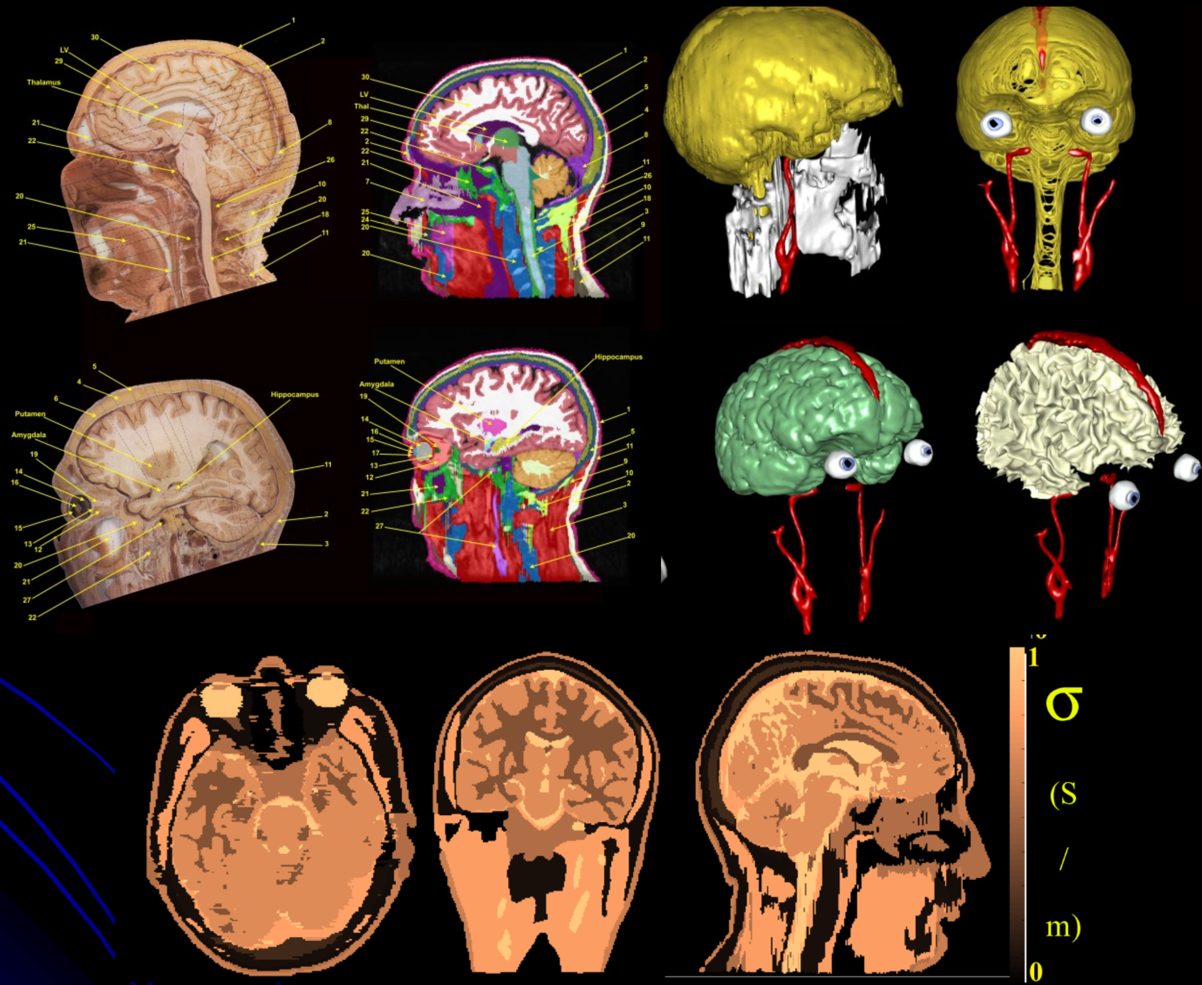

- Human Head Model Anatomically accurate with 44-tissues, 1x1x1 mm^3 resolution (Makris et al., MBEC 2009)

SAR simulations

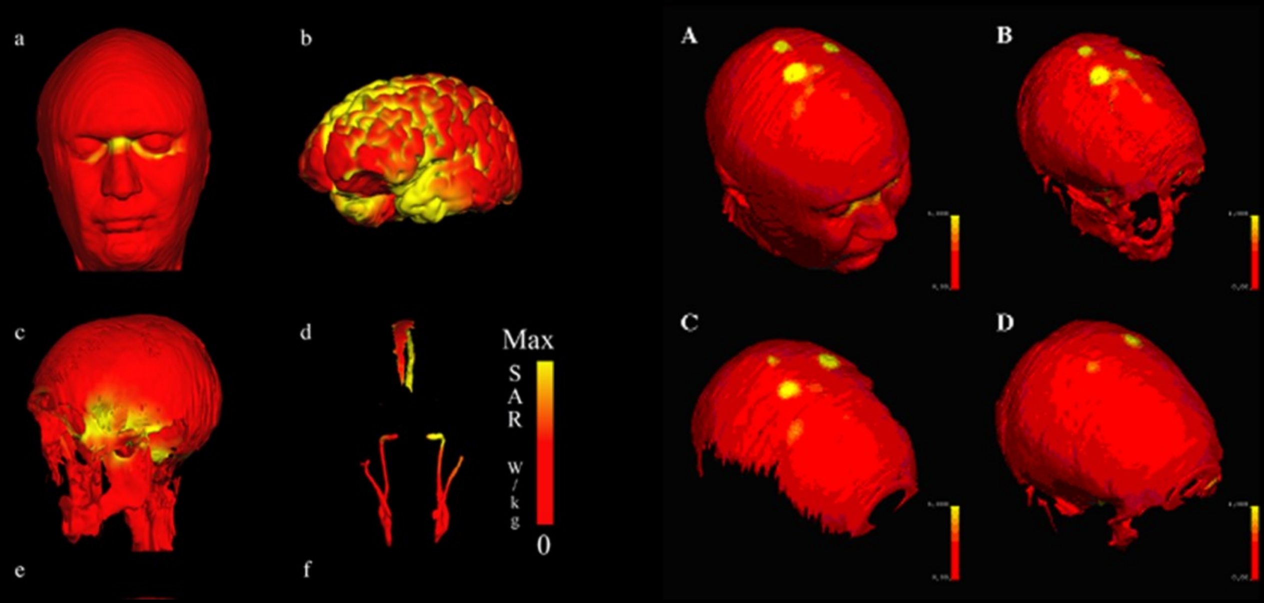

- FDTD algorithm
- Sinusoidal sources at different frequencies
- 32 electrodes + leads
- Birdcage, surface and TEM coil

Dielectric Resonance

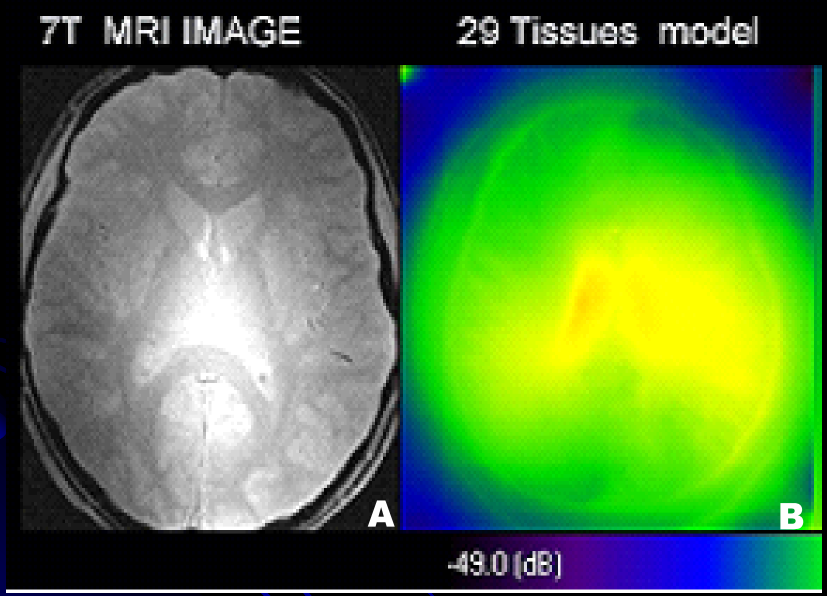

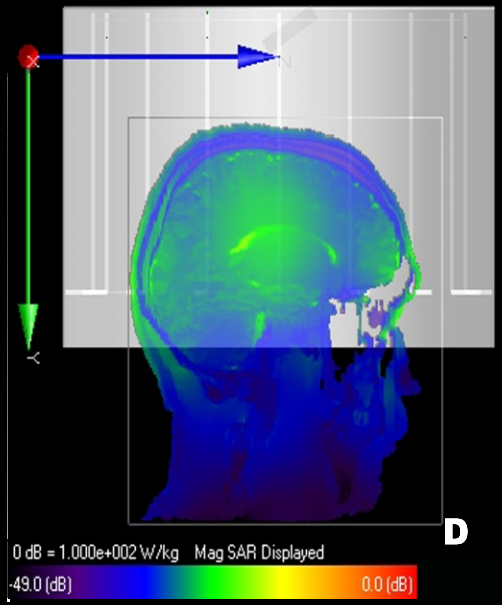

The SAR % Change with/without EEG electrodes (Birdcage)

1.5T

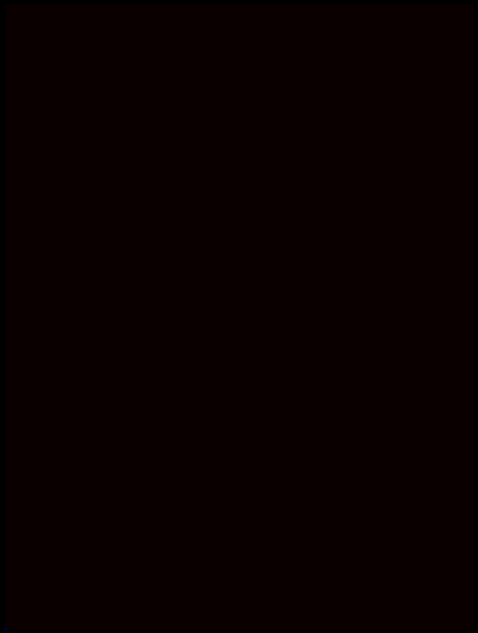

3T

6T

Variable leads resistivity

Copper | Carbon-fiber | Conductive Ink

B field

E field

Induced Currents

SAR

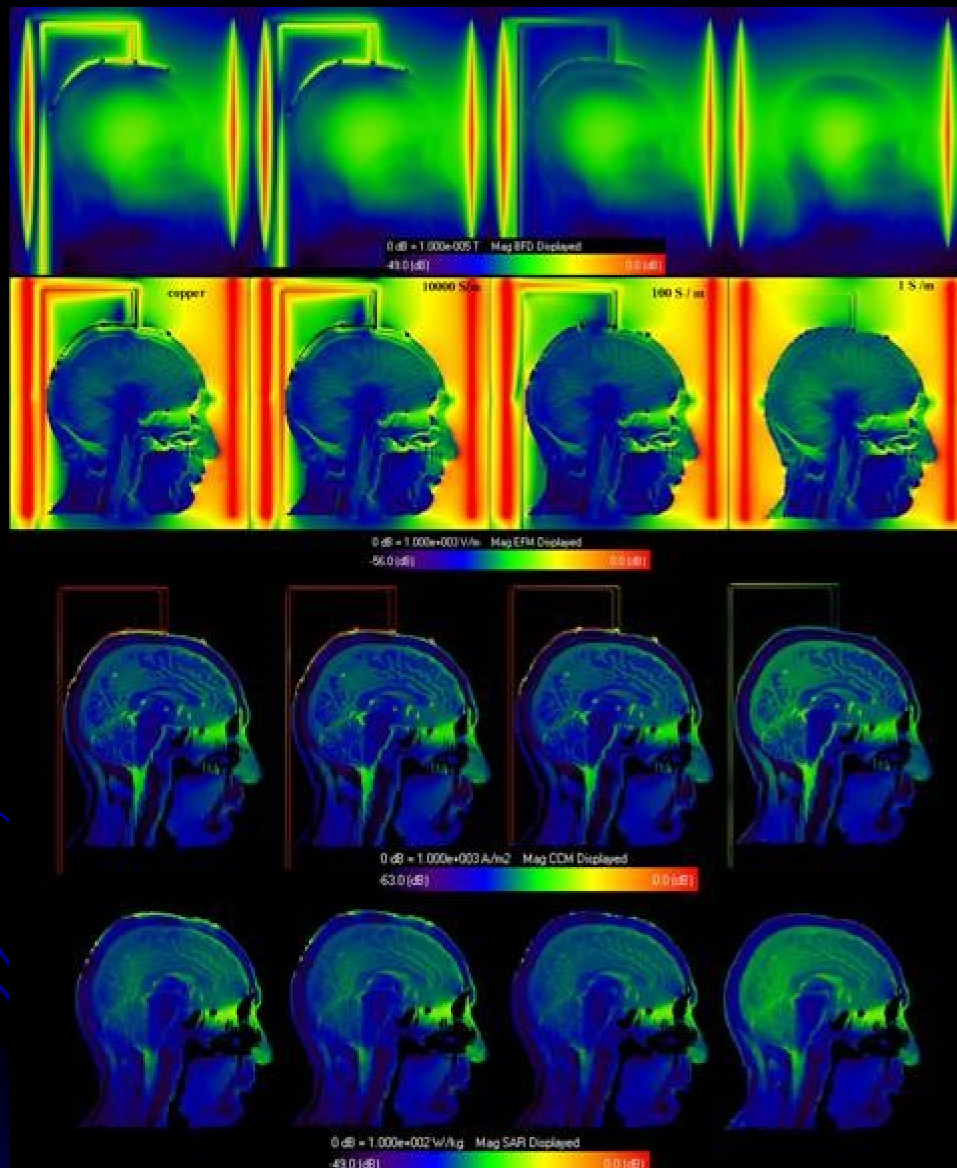

Simulations Results: effects of resistors

EEG electrodes/leads | **EEG electrodes/leads +10K**

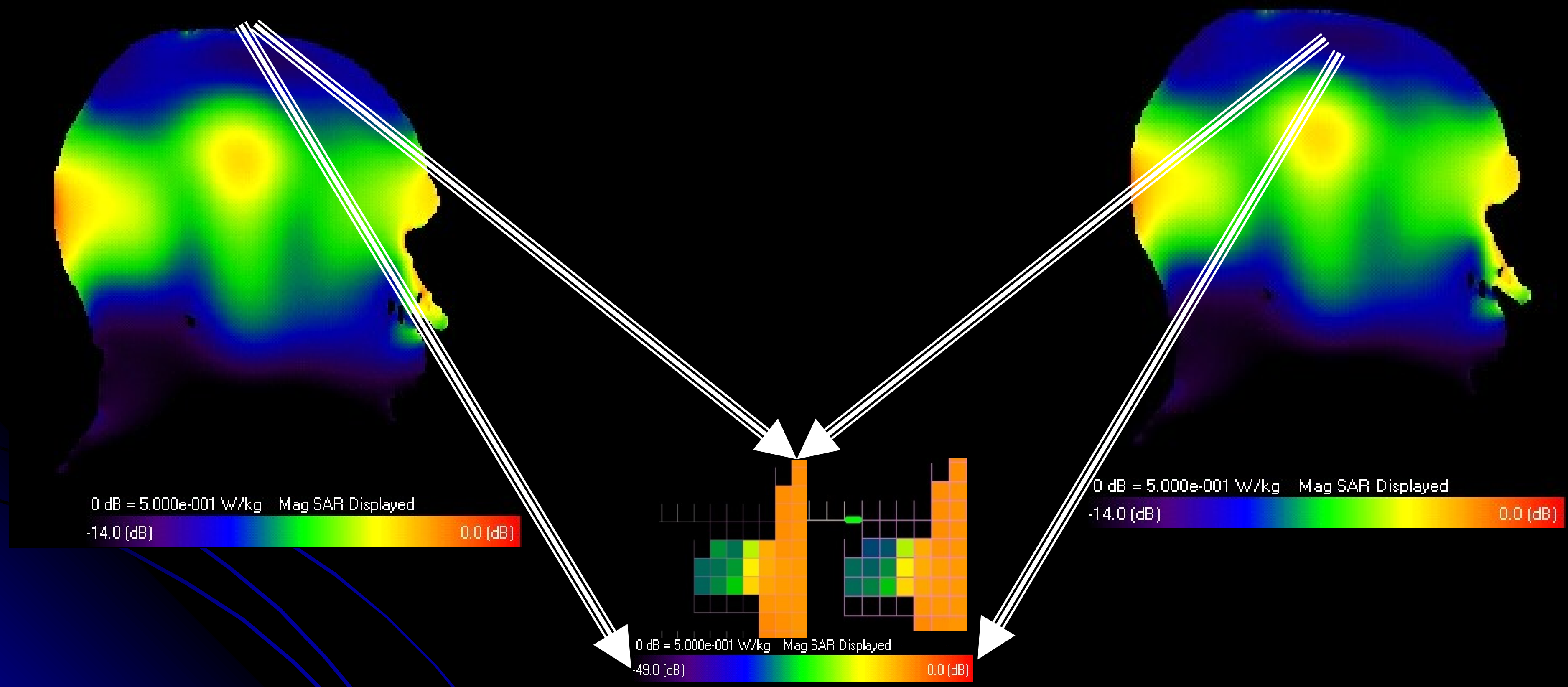

σ (S/m)	MAX	Avg.	Efficiency
EEG elec/leads	0.84	0.09	49.21%
EEG elec/leads +10K	0.84	0.09	49.21%

Temperature Measurements at 7T

- 7T whole body system retrofitted with a Siemens Sonata console
- High power TSE sequences

- Luxtron 3100 Fluoroptic Thermometer device with 4 MRI compatible probes (0.5 ^{o}C resolution)

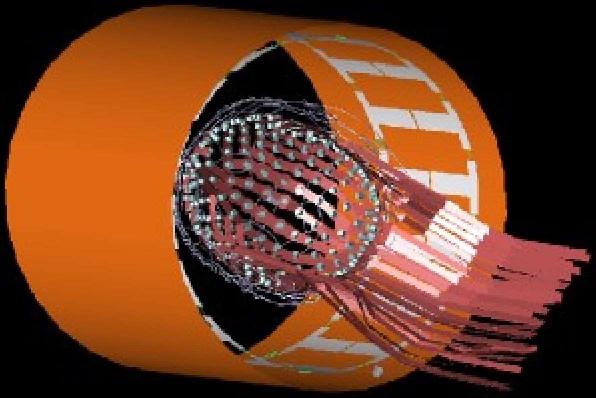

- C.HE.M.A: Conductive HEad Mannequin Anthropomorphic Phantom
  - Anatomically accurate with head model
  - Composition: 4.5lt. water, 135gr. agarose, 40.5gr NaCl

The "InkNet"

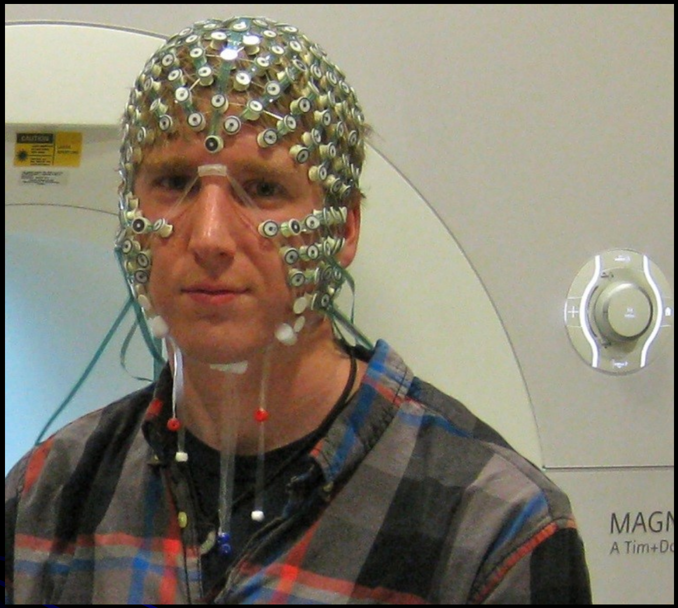

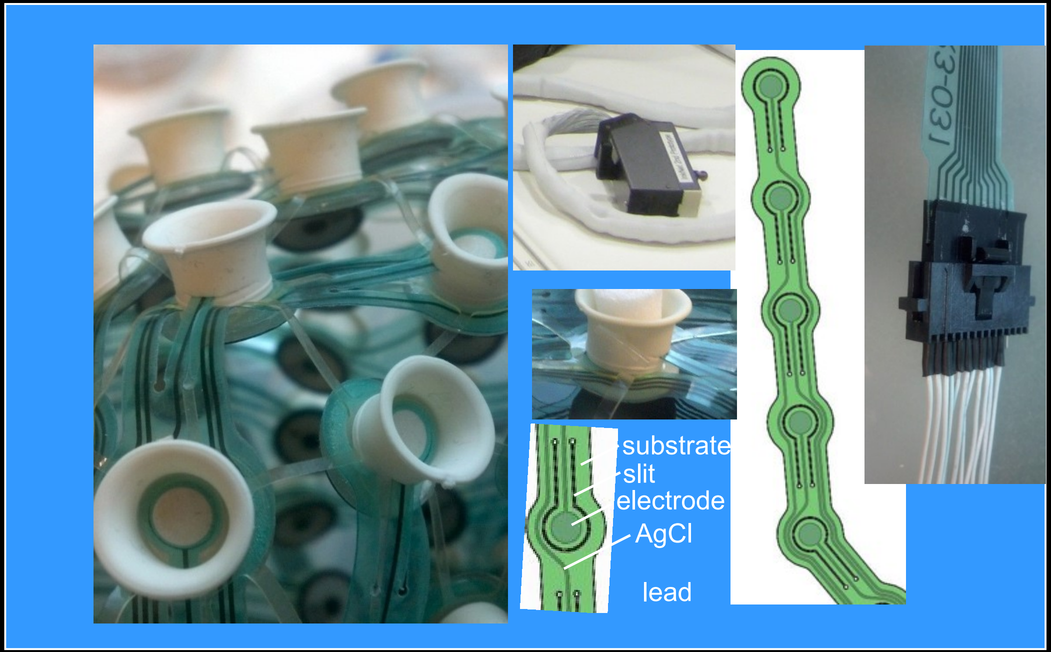

- 32 flexible circuit boards
- 256 electrodes + REF + GND
- Cup electrode design
- PTF traces for RF transparency

No Electrodes vs. InkNet vs. Standard Net

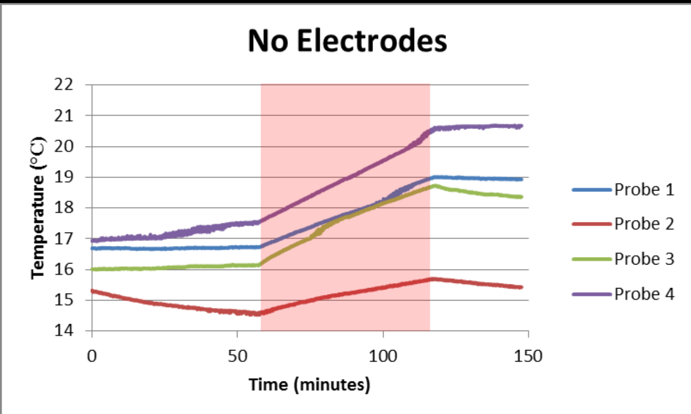

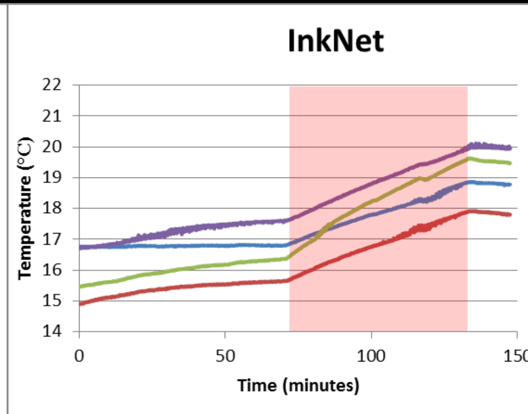

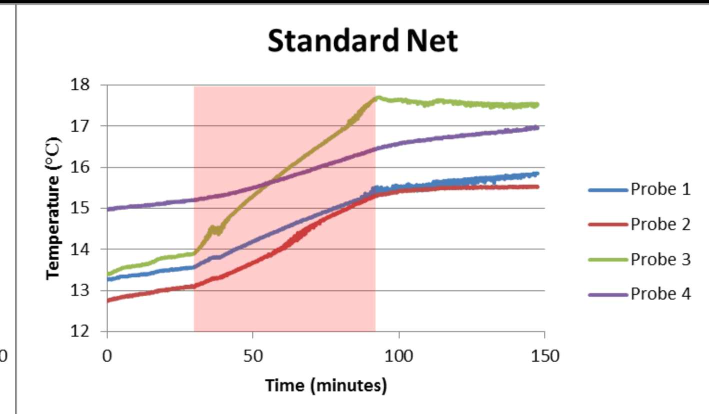

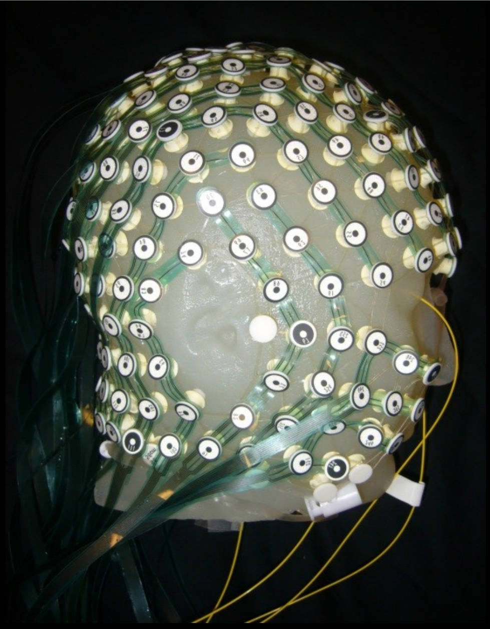

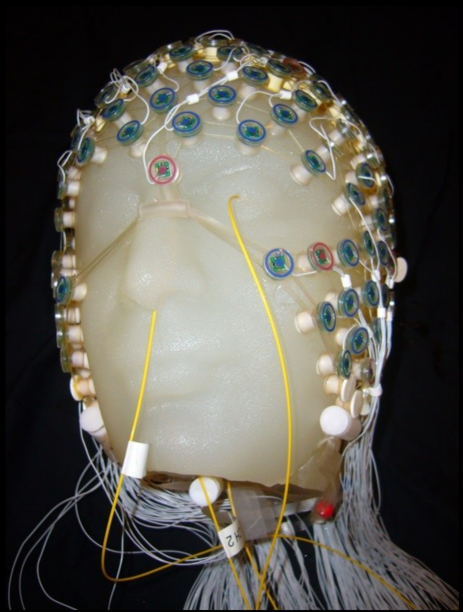

2. fMRI quality: Testing the EEG cap on the BOLD signal with the Eccentricity Map

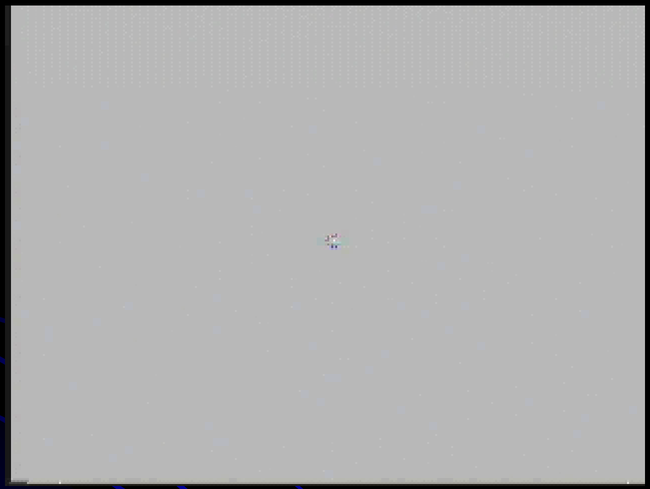

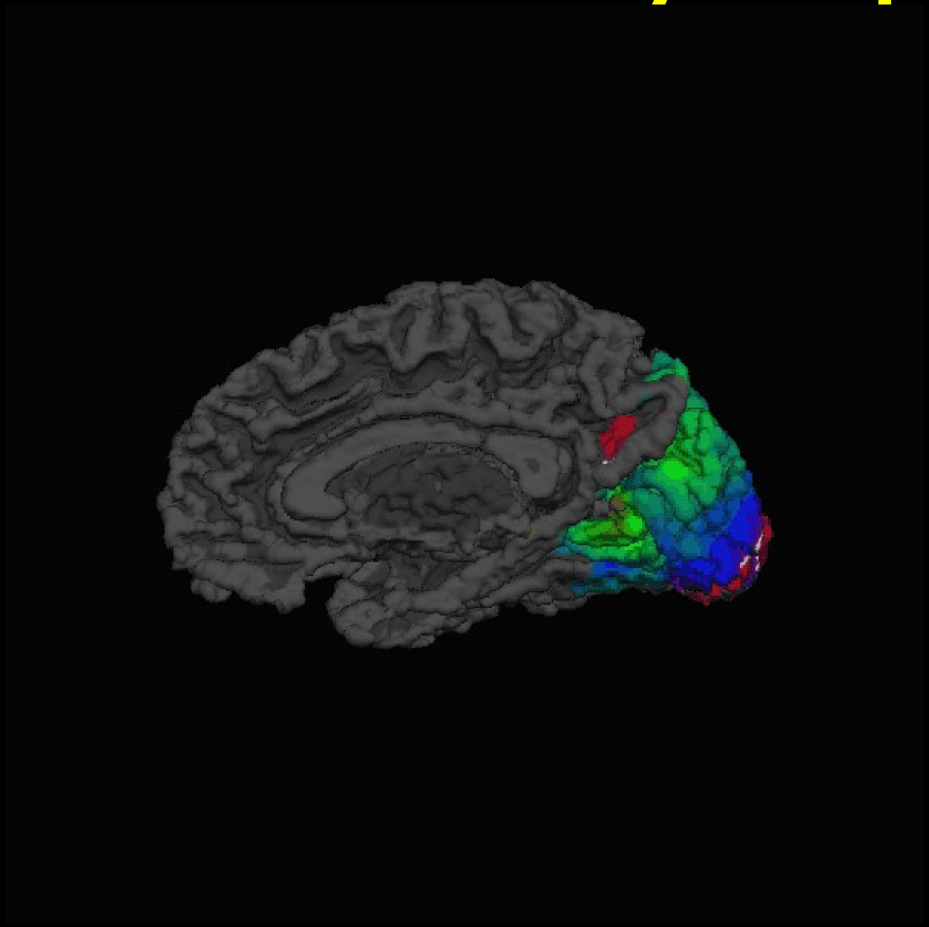

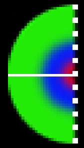

Visual Field Eccentricity Mapping on Cortex

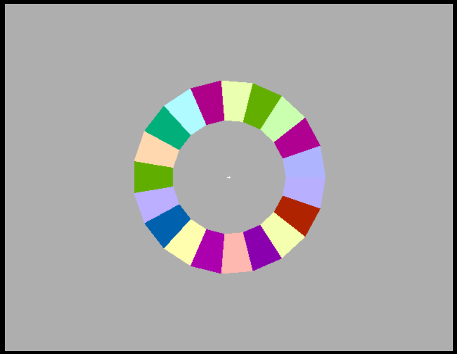

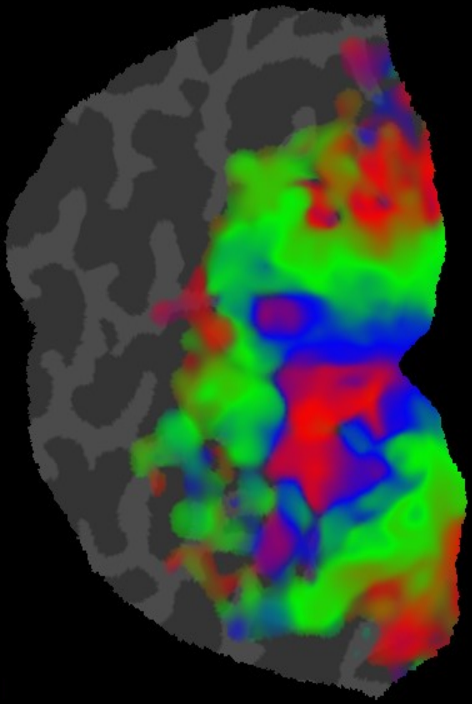

Sereno et al., 1995

Retinotopy with/without electrodes

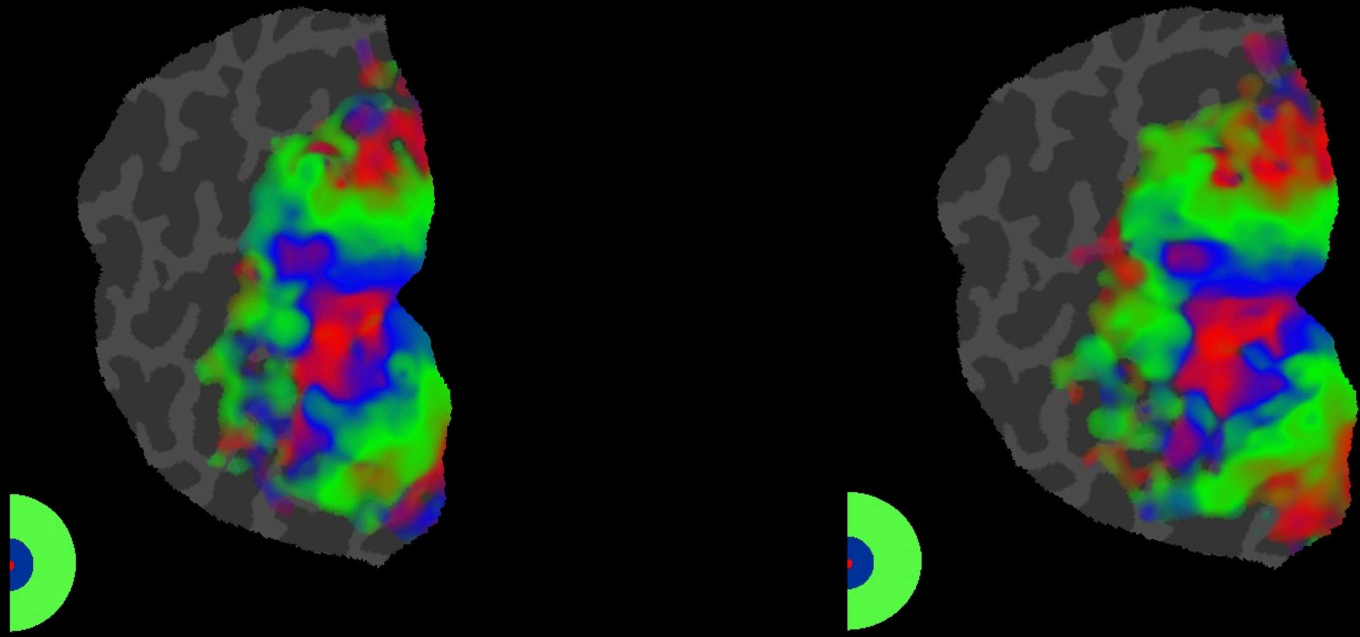

Retinotopy with/without electrodes

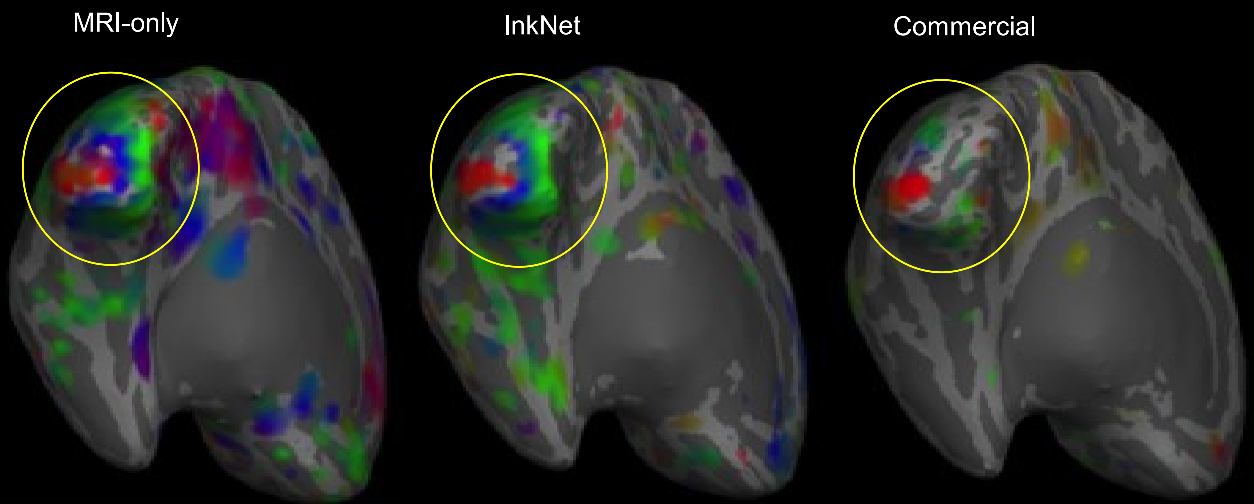

Eccentricity maps displayed on inflated medial occipital cortex surface reveal considerably greater signal loss from presence of commercial net than InkNet when compared to MRI-only (red, blue, green palette indicates BOLD response to increasing stimulus eccentricity).

3. Noise induced on the EEG recordings

- Static Magnetic Field:
  - ✓ Physiological noise (heart, breathing, muscular, etc.)
  - ✓ Room vibration noise (helium pump, sounds, etc.)
- Switching Magnetic Gradient Field
- RF interference

Faraday's Induced Noise

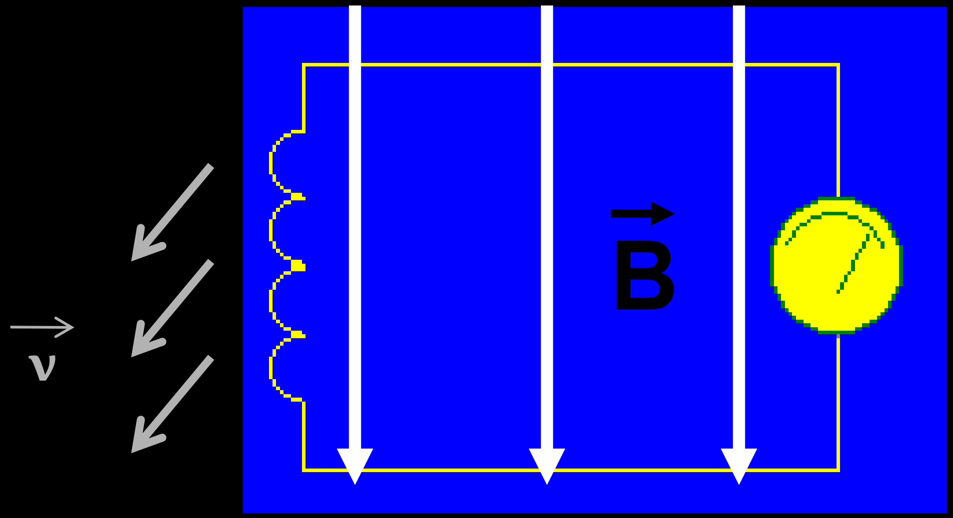

$$\varepsilon = N \frac{\partial \phi}{\partial t}$$

- Faraday's induced noise:
  - Motion of the EEG electrodes and leads generates noise
- Physiological Motion is Primary Noise Source
  - heart beat (ballistocardiogram), breathing, subject motion

Pulse Artifact Subtraction (Allen, 1998)

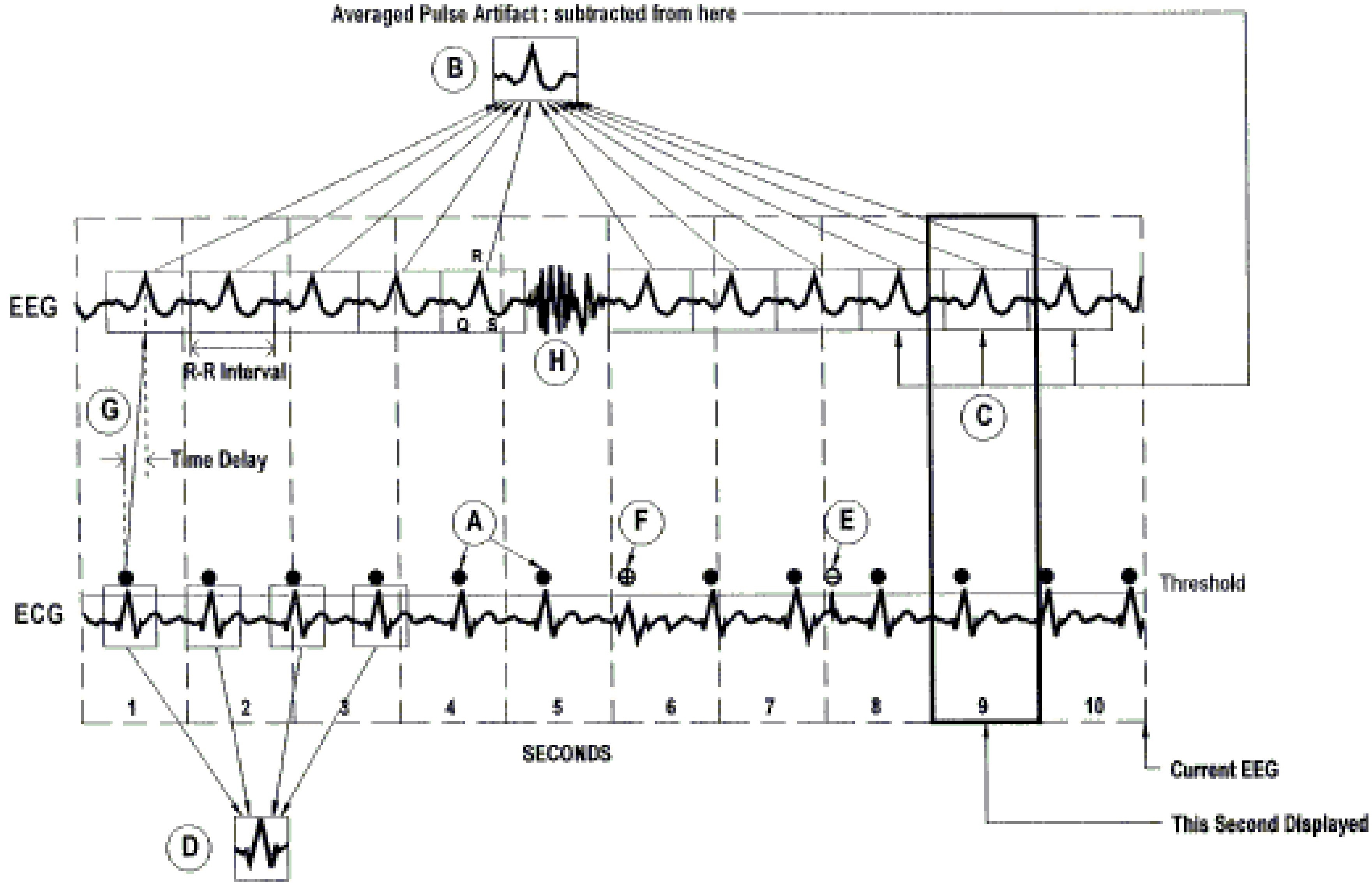

Other Noise Cancellation Techniques

- Synchronization of the EEG sampling with gradient switching (Goldman et al., 2000; Anami et al., 2003; Mandelkow et al).
- ICA cancellation methods (Mantini et al., 2007)
- Optimal basis set (Niazy et al., 2005)
- Frequency based methods (Zakharov et al., 2007)
- Adaptive filtering methods (Sijbers et al., 1999 and Wan et al., 2006)

Software solution: Adaptive Noise Cancellation

- Use a *motion sensor* signal to remove noise
  - Exogenous reference signal uncorrelated with underlying EEG signal
- Time-varying algorithm
  - e.g., track changes in changes in impedance, electrode position, etc.
- Implementable in real-time

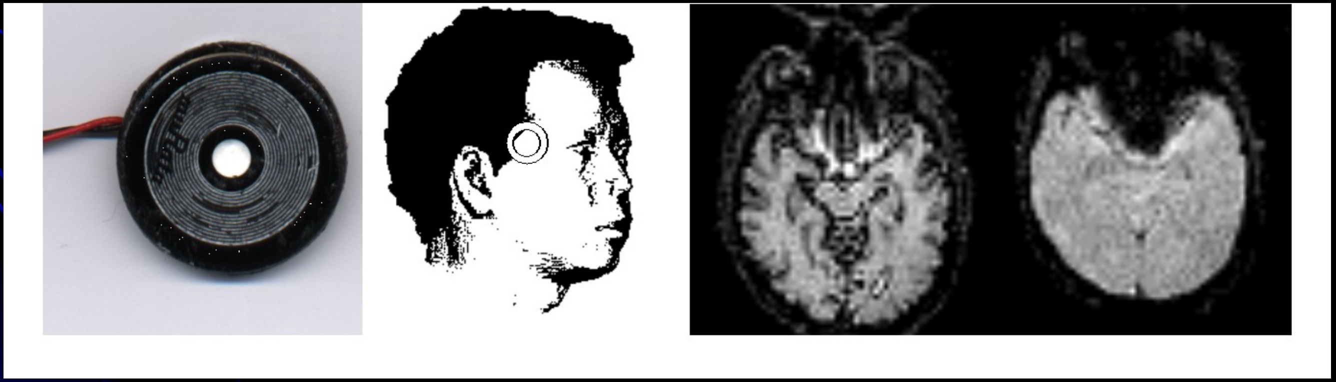

Adaptive Filter Algorithm

- Observed signal

$$y(t) = s(t) + n(t)$$

True underlying EEG → $s(t)$

Induced noise → $n(t)$

- Linear time-varying FIR model for induced noise

$$n(t) = \sum_{k=0}^{N-1} w_k(t) m(t-k)$$

FIR kernel → $w_k(t)$

Motion sensor signal → $m(t-k)$

Adaptive Filtering Algorithm

- Estimate filter taps $w_h(t)$ recursively using Kalman filter algorithm

$$\hat{w}_h(t+1) = \hat{w}_h(t) + k_h(t)\left(y(t) - \sum_{k=0}^{N-1} \hat{w}_k(t) m(t-k) \right)$$

- Remove estimated noise signal, yielding clean EEG

$$\hat{s}(t) = y(t) - \sum_{k=0}^{N-1} \hat{w}_k(t) m(t-k)$$

Piezoelectric Motion Sensor

- Adaptive ballistocardiogram noise filtering (Bonmassar et al., NeuroImage 16, 1127–1141, 2002)
- Position: Temporal Artery

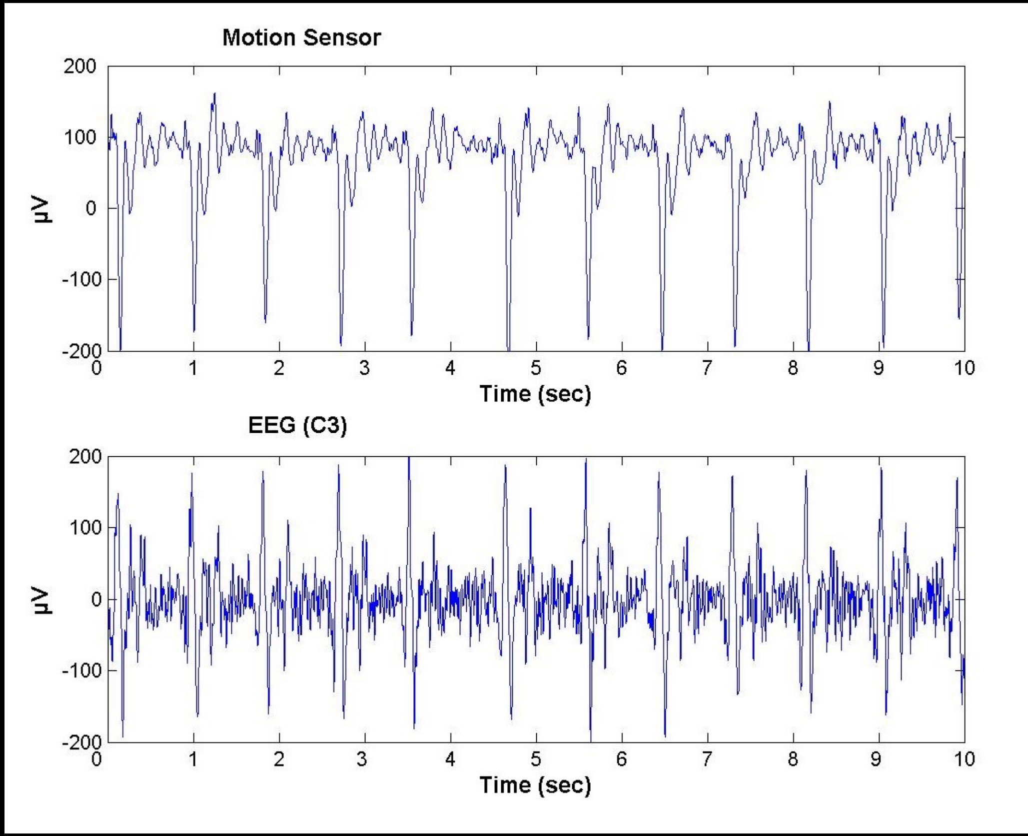

Results: VEPs

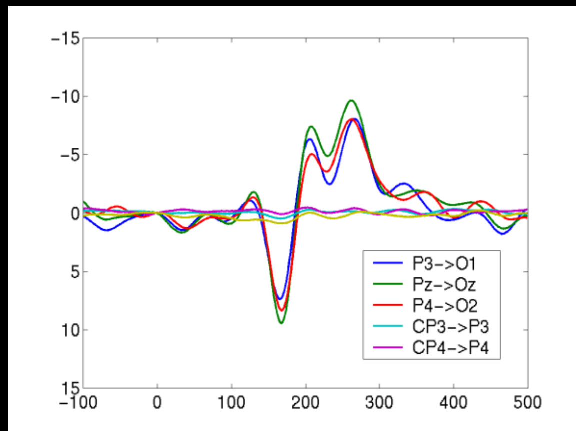

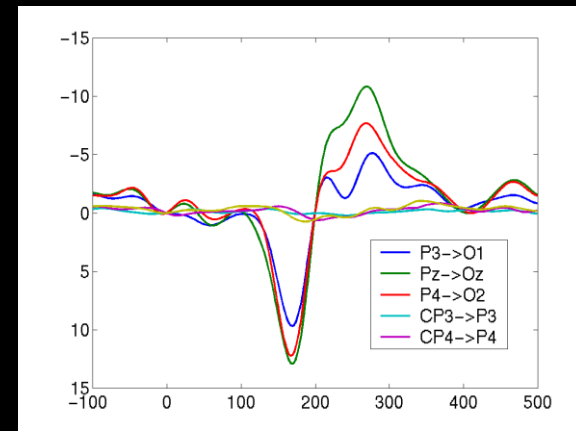

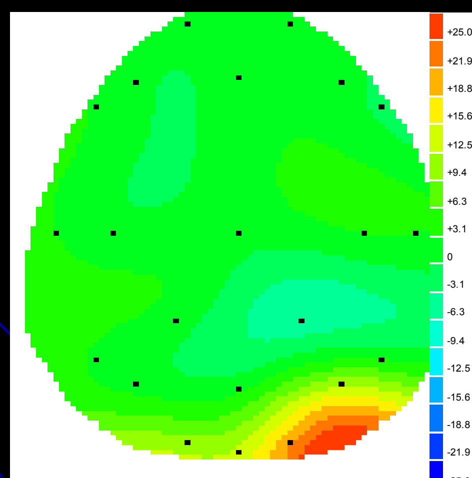

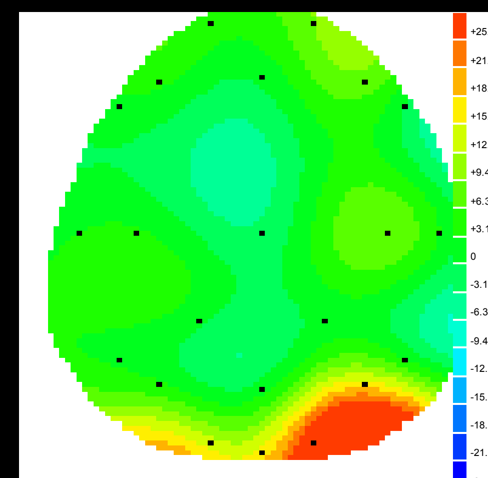

Outside Magnet

Inside Magnet

Spatiotemporal Dynamics of Brain Activity following visual stimulation

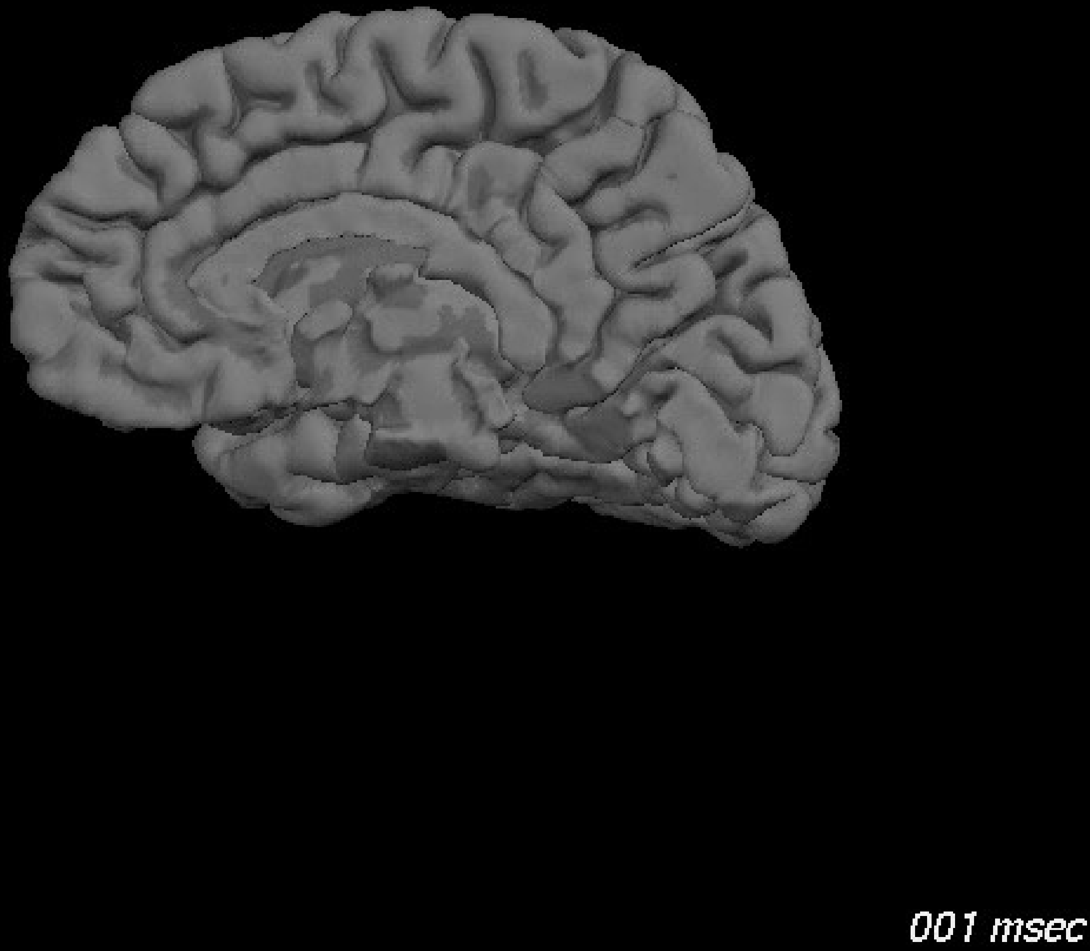

Any natural basis for artifact?

Record BCG artifacts in scanner with subjects at rest, awake, eyes open

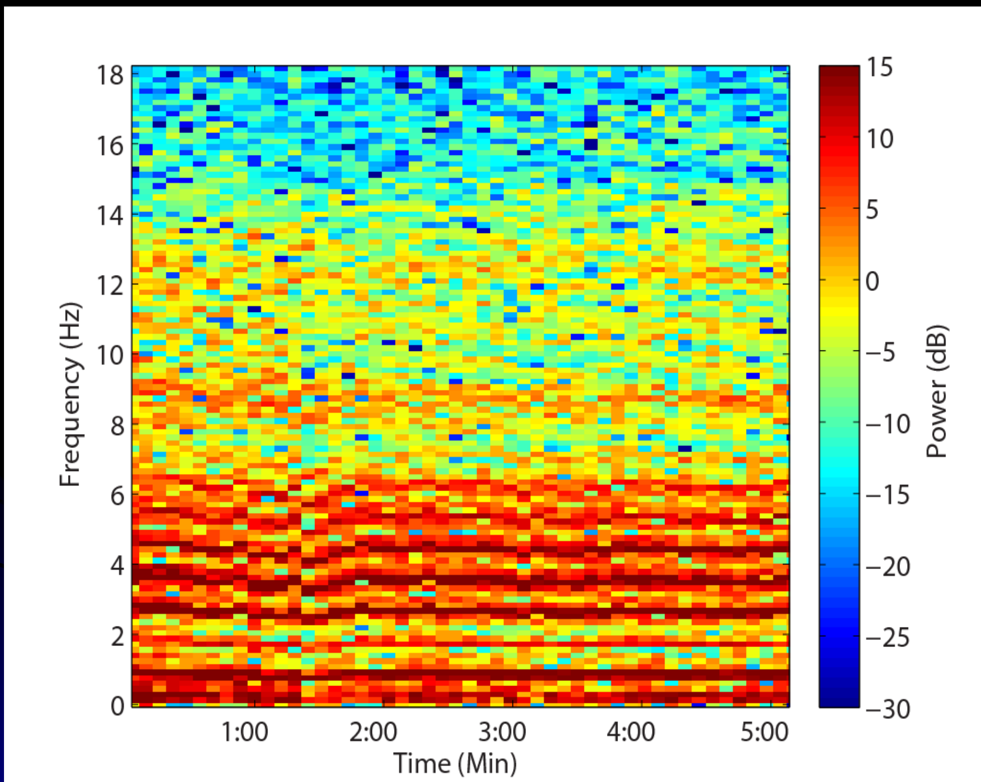

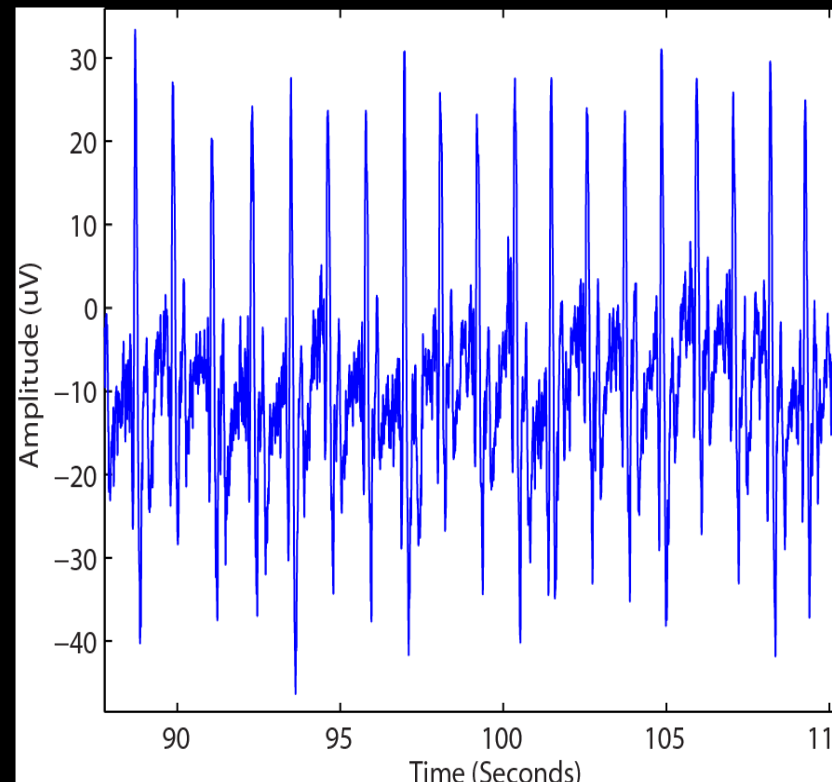

Posit that BCG has a Harmonic Basis

Approach: Model this Template and Regress out Artifact

Krishnaswamy, et. al (IEEE EMBC 2013)

Model and Approach

Observation $y_t = s_t + v_t$

Harmonic BCG Artifact

$$s_t = \mu_o + \mu_1 t + \sum_{r=1}^{R} A_r \sin(\omega r t) + B_r \cos(\omega r t)$$

$$\boldsymbol{\beta} = [\mu_o \;\; \mu_1 \;\; A_1 \; \ldots A_N \; B_1 \;\; \ldots B_N]$$

Unknowns:
Fundamental Frequency, Harmonic Amplitudes

Oscillatory Brain EEG: Autoregressive Model

$$v_t = \sum_{k=1}^{P} a_k v_{t-k} + \epsilon_t$$

$$\epsilon_t \sim \mathrm{N}(0, \sigma_\epsilon^2)$$

$$\boldsymbol{\alpha} = [a_1 \ldots a_P]$$

Unknowns:
AR Coefficients, Residual Variance

BCG Removal Problem Becomes Parametric Estimation Problem
Solve for parameters in real-time with local maximum likelihood methods

Krishnaswamy, et. al (IEEE EMBC 2013)

Delta Band On/Off Pattern

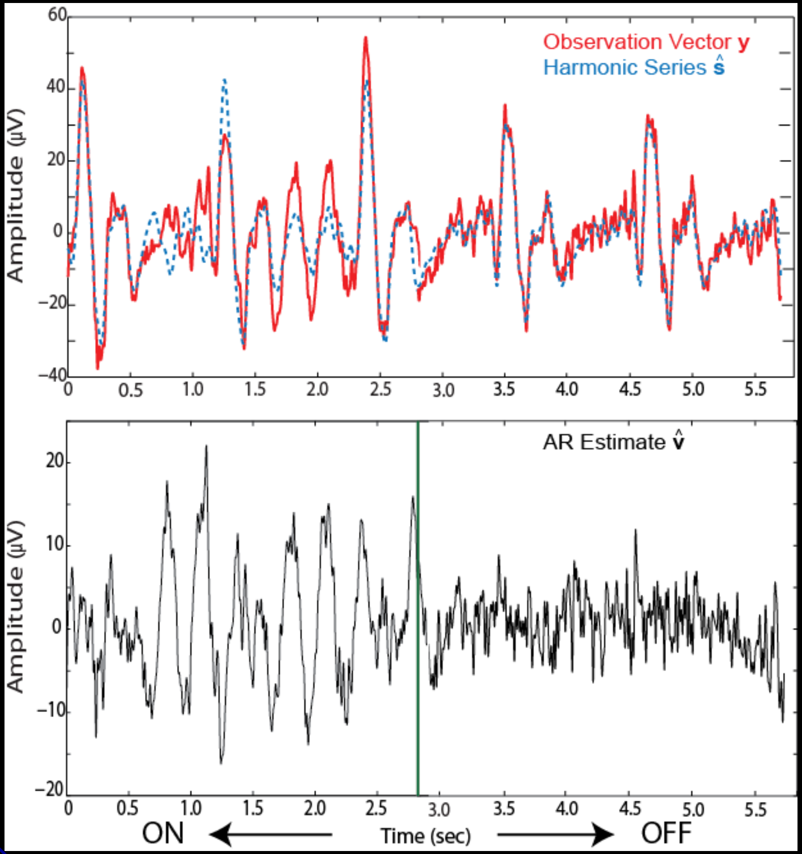

Observation Vector And Harmonic Fit

Estimate of True Brain Generated EEG

Estimated EEG has correct 3-4 Hz ON/OFF pattern

Krishnaswamy, et. al (IEEE EMBC 2013)

4. Early BOLD spike response

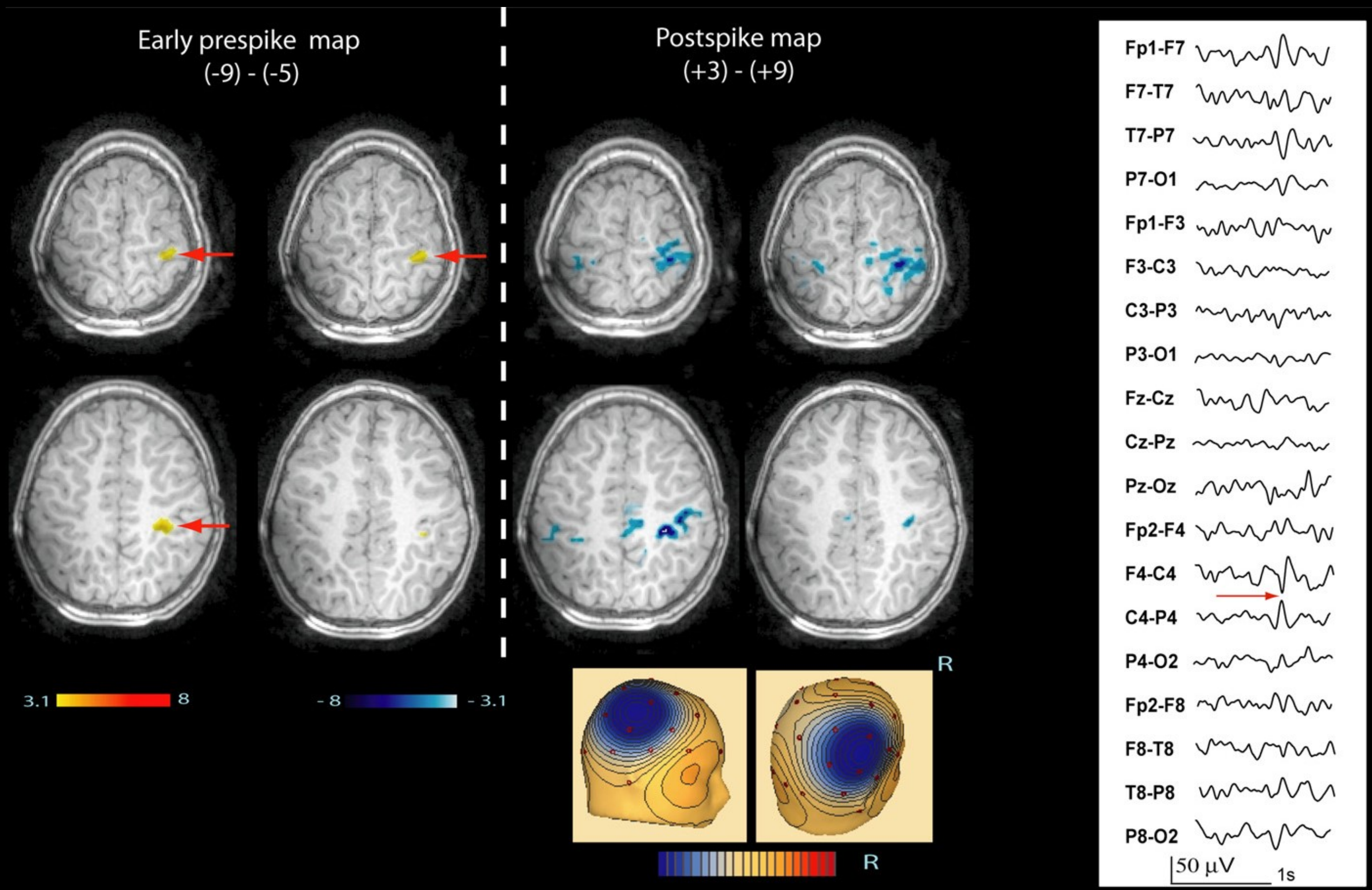

Jacobs et al., Neuroimage 2009

BOLD Response to Epileptic Spikes at 1.5T and 3T

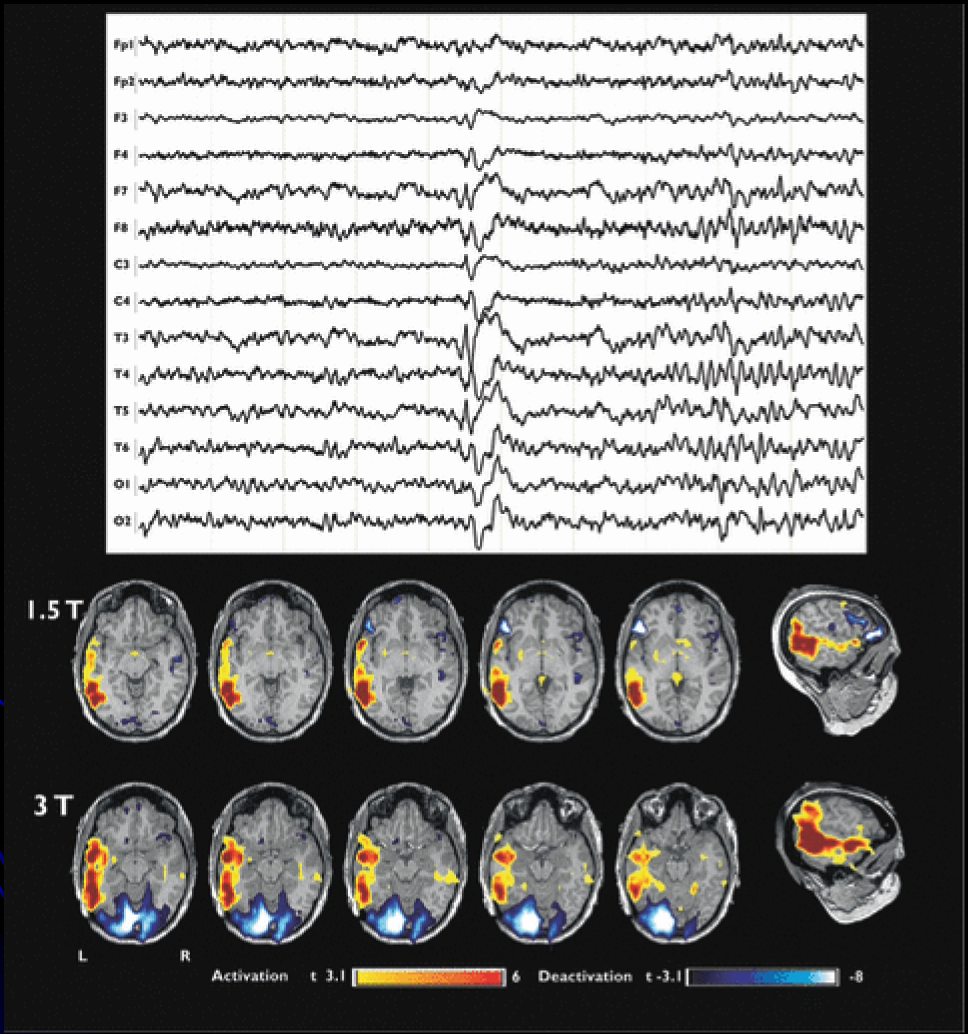

Gotman et al. 2011

BOLD Signal at 7T

Jon Polimeni, MGH.

7T
0.75mm isotropic
Single shot EPI
32ch
R=3 Grappa

Average of 10 shots shown

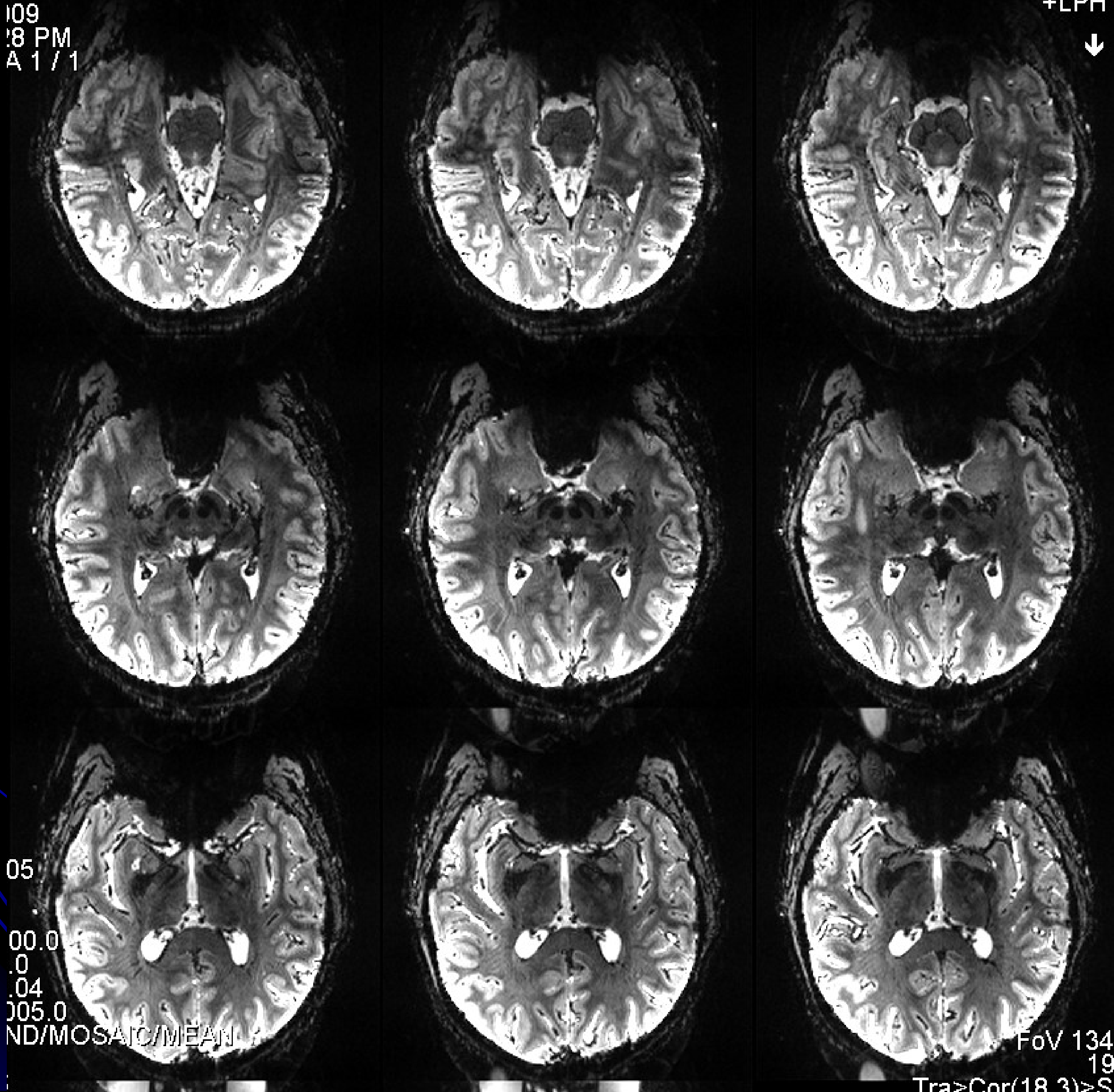

0.75mm 7T

0.5mm isotropic

Single shot EPI

32ch
R=4 Grappa

Average of 10 shots shown

0.5mm 7T

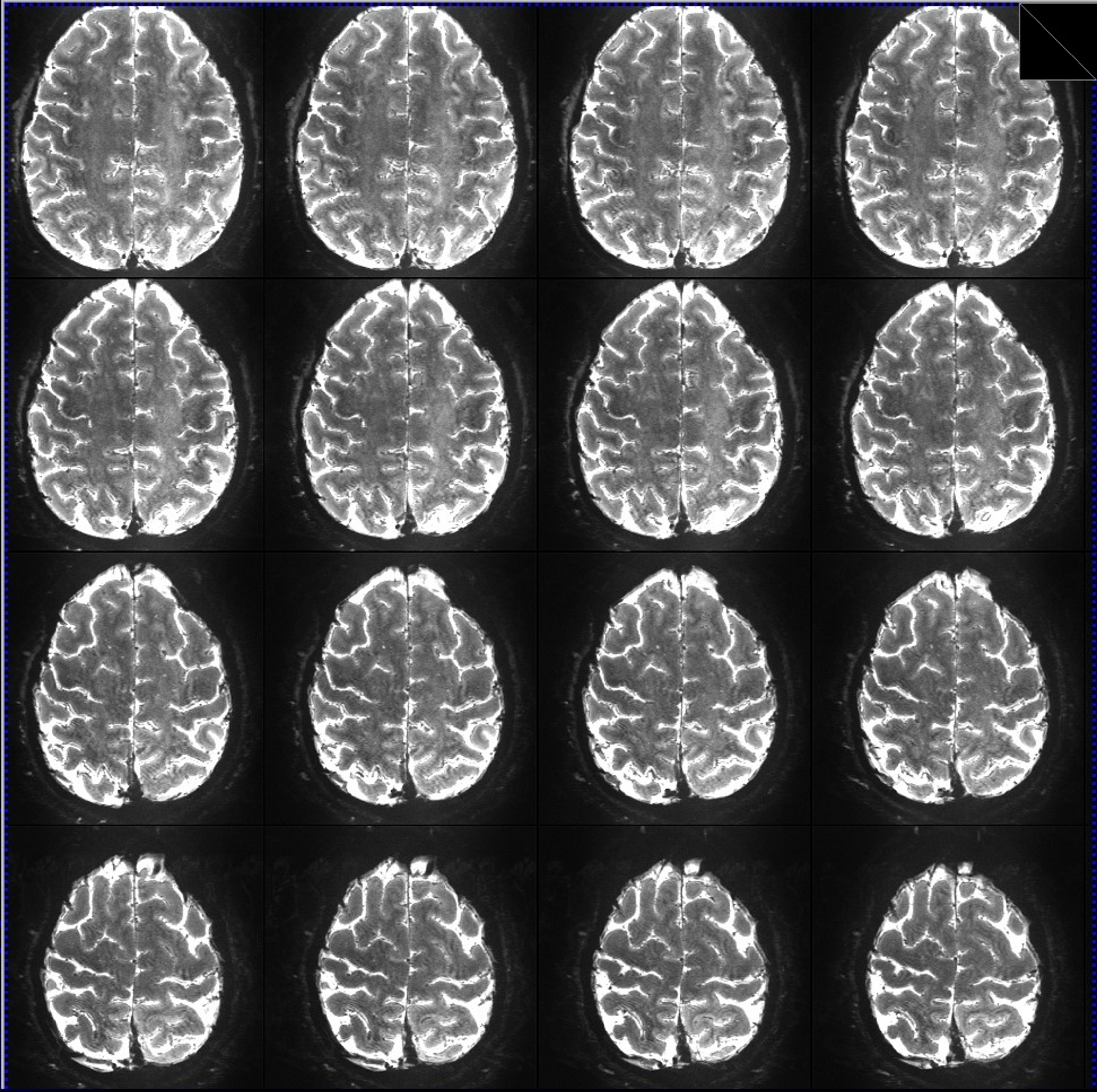

Resolution Stimulus

goal: imposed desired activity pattern on V1 surface

Jon Polimeni, MGH.

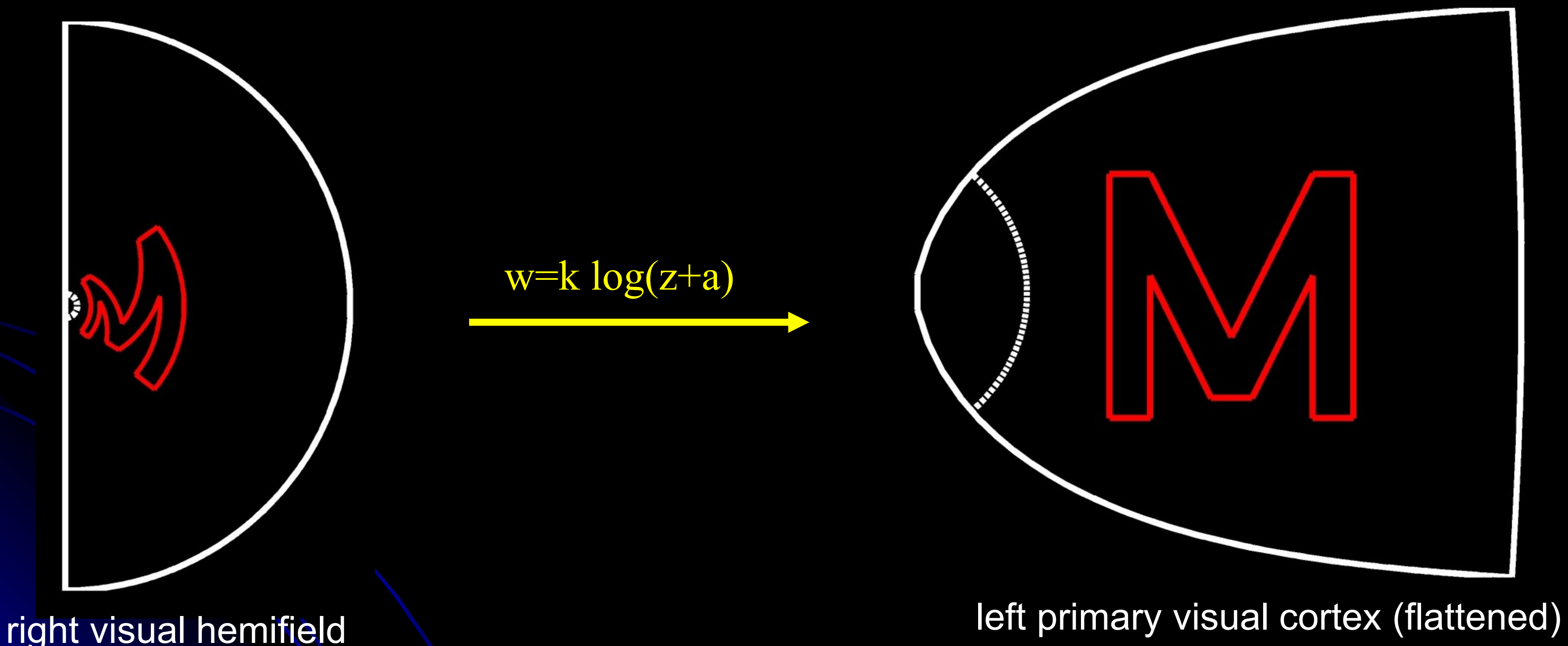

resolution stimulus

stimulus condition A

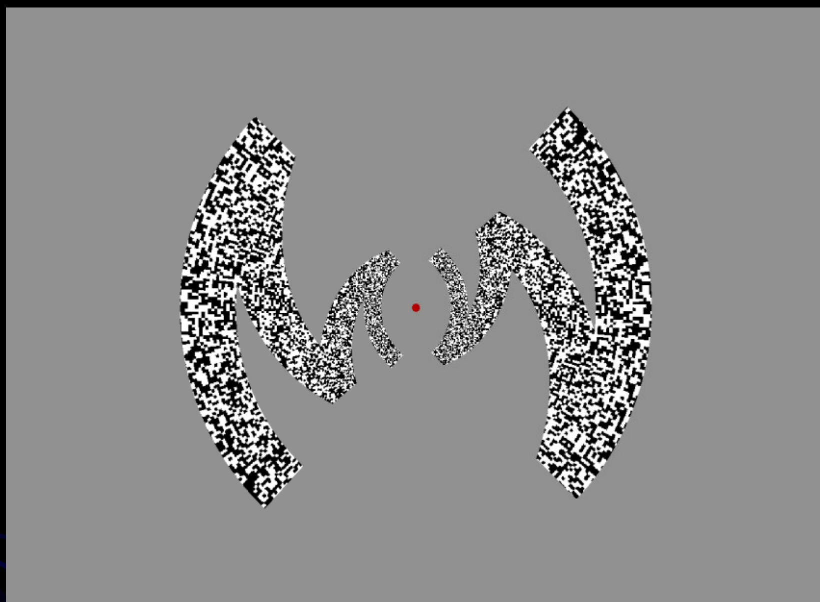

stimulus condition B

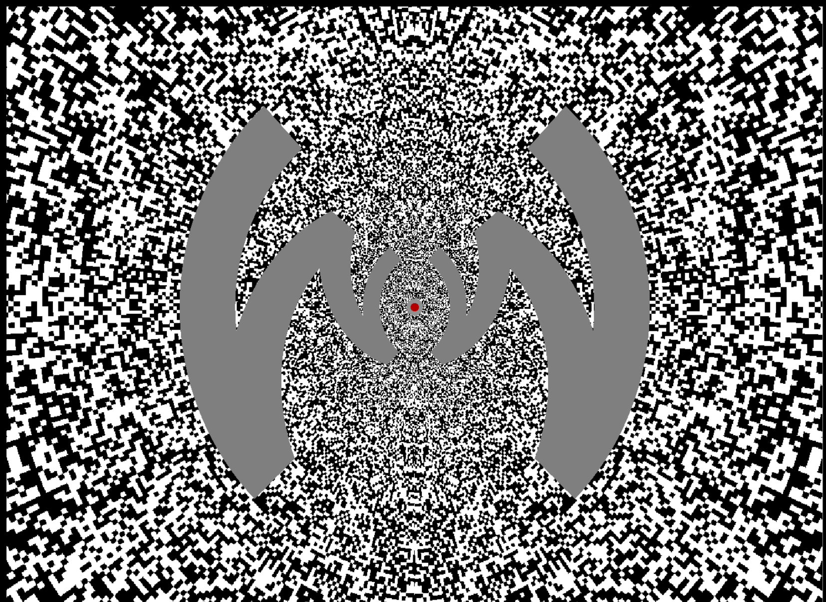

Jon Polimeni, MGH

- counterphase flickering (8 Hz) scaled spatial noise pattern
- fixation task to minimize blurring due to eye movements
- block design presentation: two stimulus conditions plus rest, 5min total

View activation on inflated surface

5 Minute block design

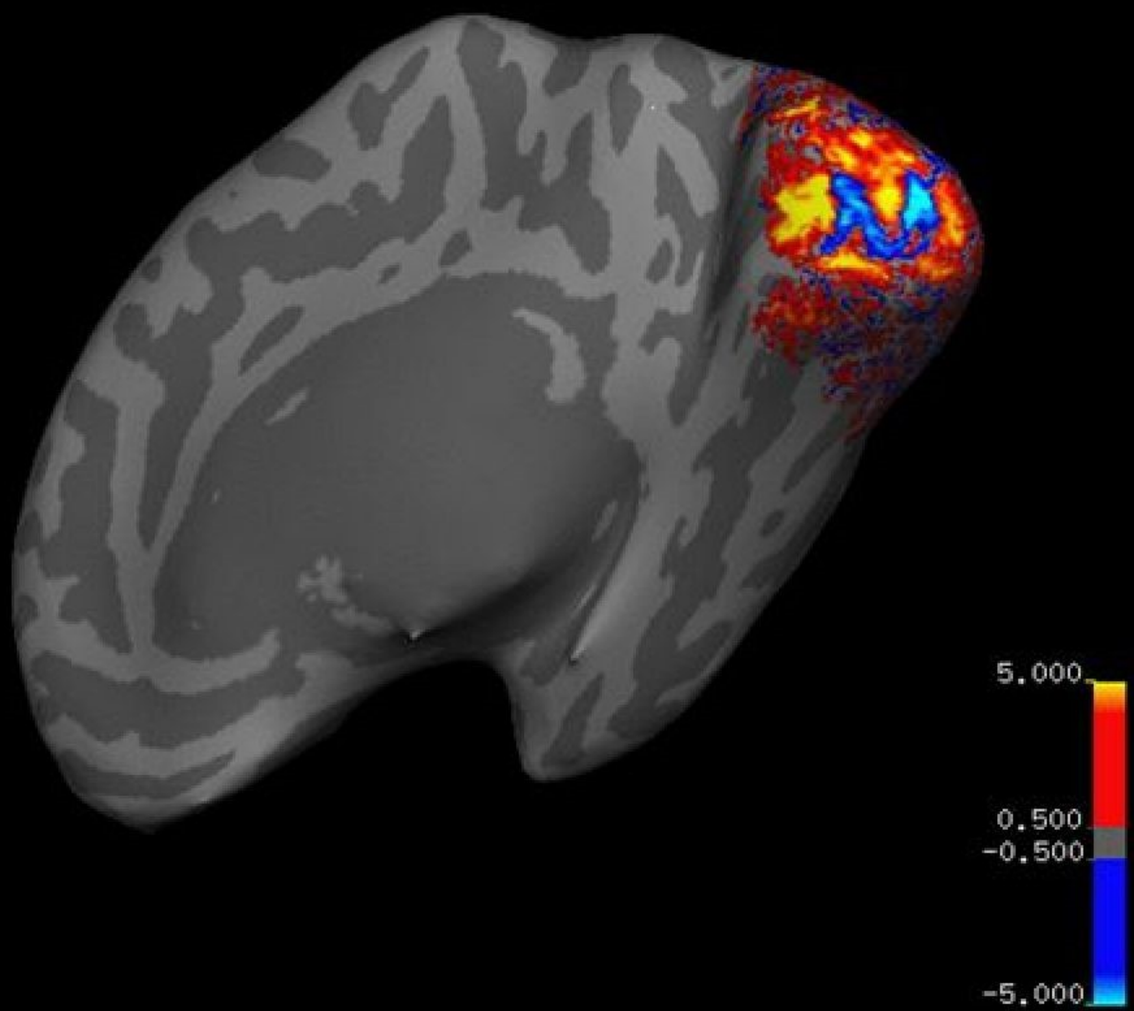

Jon Polimeni, MGH

Generate a cortical surface at each depth…

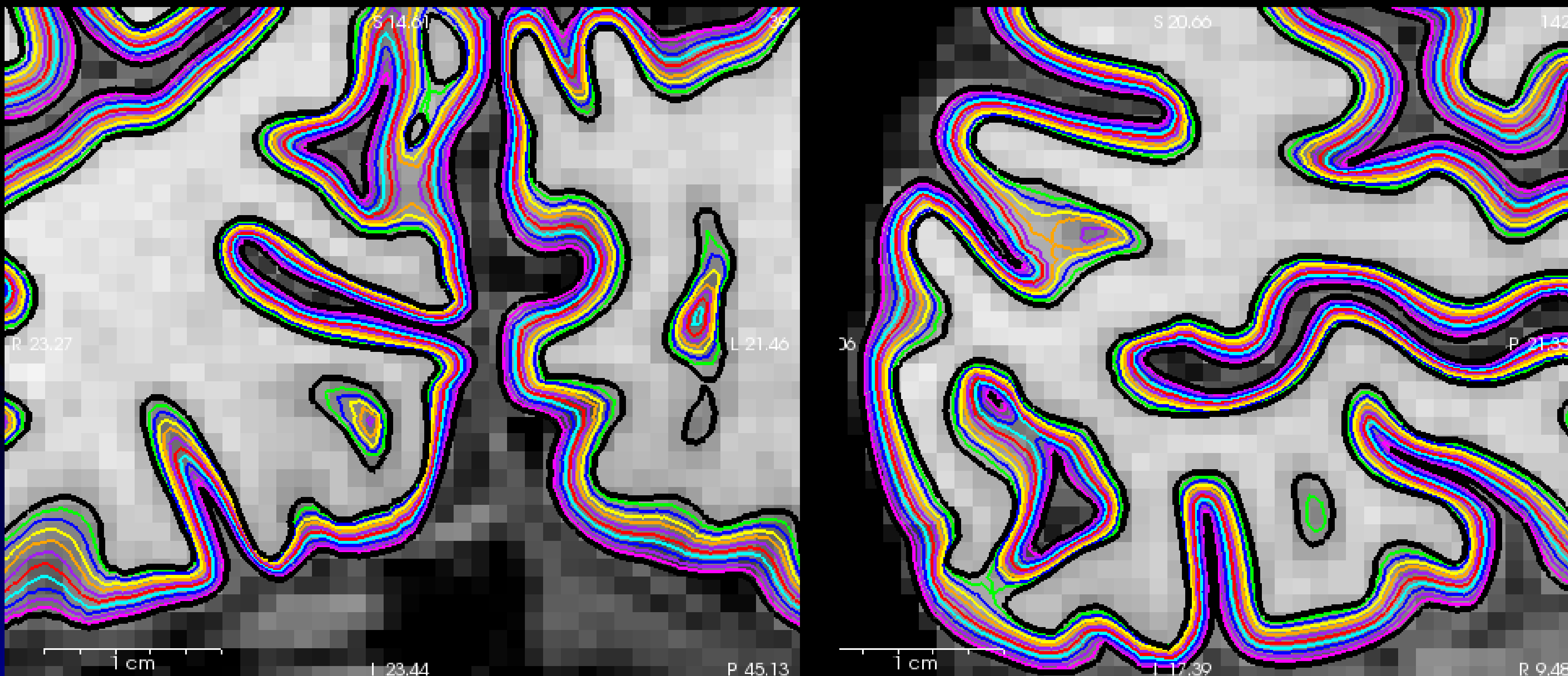

Bruce Fischl, MGH

View activation pattern from voxels thru each of the many cortical surfaces.

TA: 5 min, 24 sec

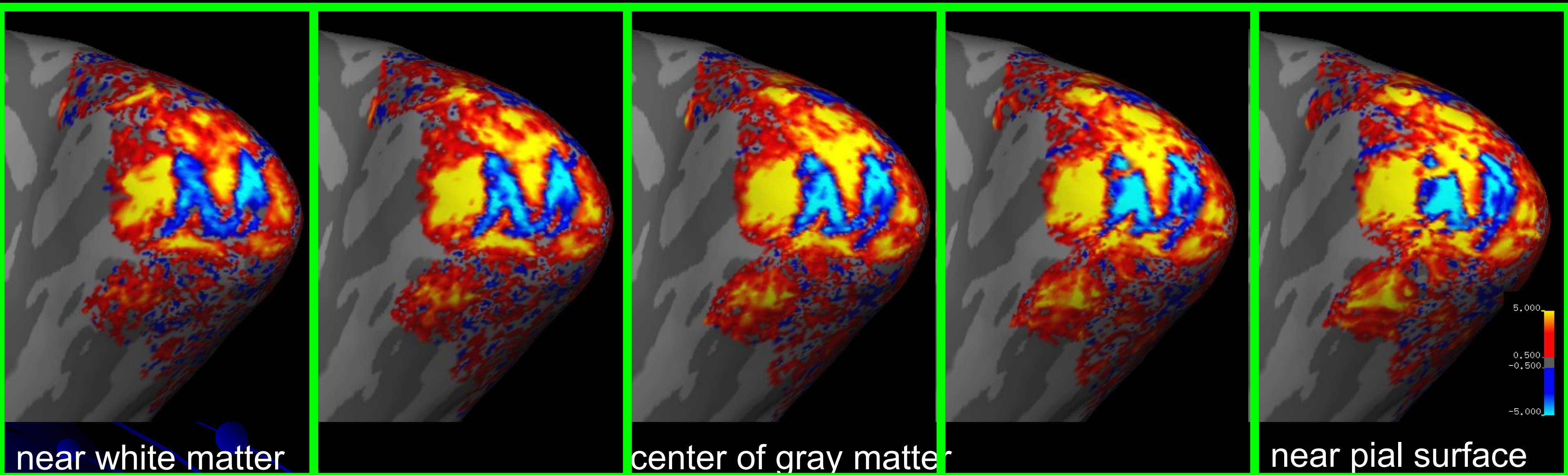

Resolution Pattern Degrades with Proximity to Pial Vessels

EEG/fMRI to study Anesthesia

Purdon et al. 2009 MGH

EEG/fMRI/Propofol

- Graded Propofol Infusion
- Cardiac-Gated fMRI (Brainstem)
- EEG (40 Hz ASSR)
- Behavioral Task (Consciousness)
- Blood Gas (CO_2)
- Blood Propofol Level
- Physiological Data ($EtCO_2$, ECG, BP, SpO_2)

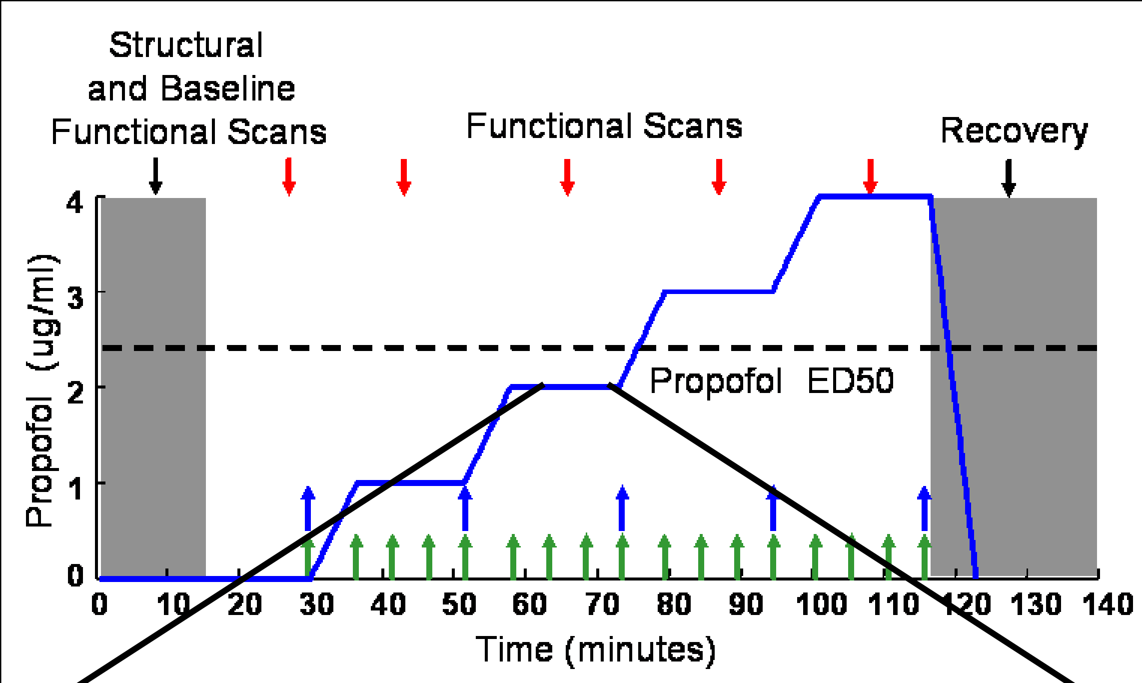

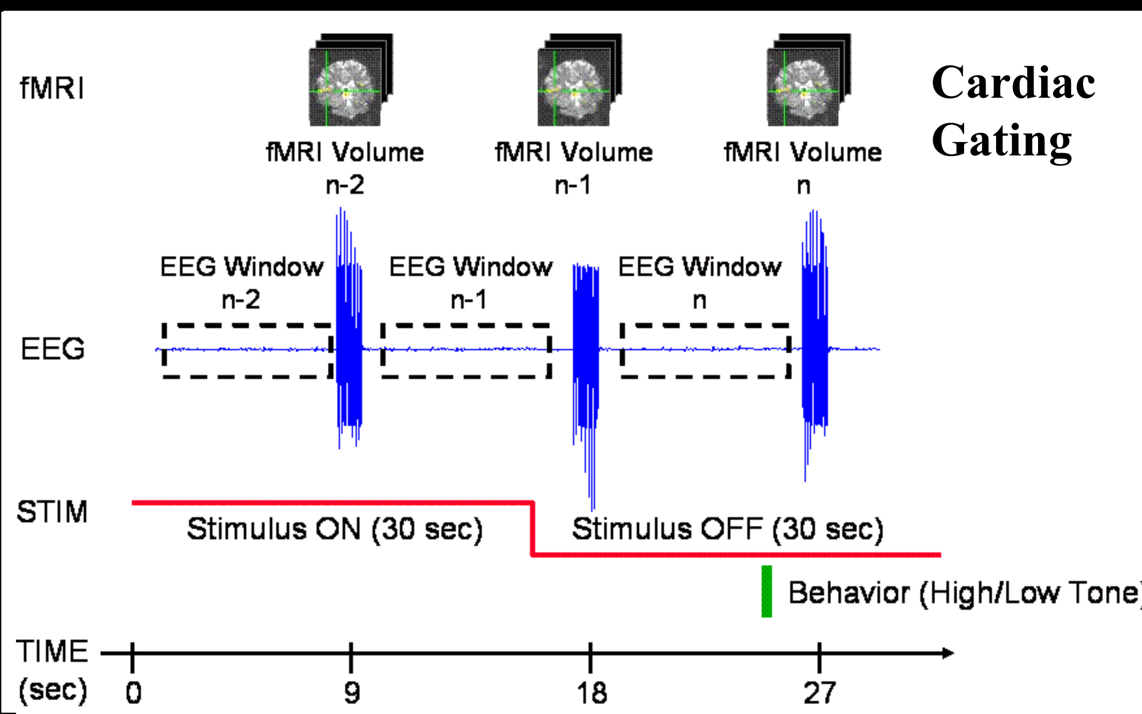

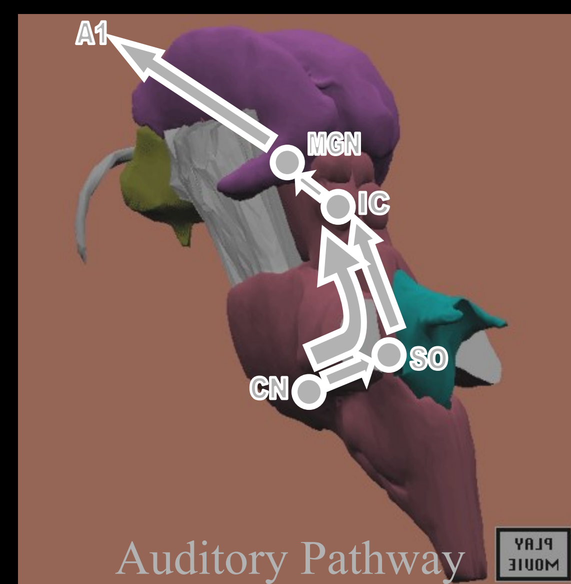

Auditory Evoked Potentials and fMRI

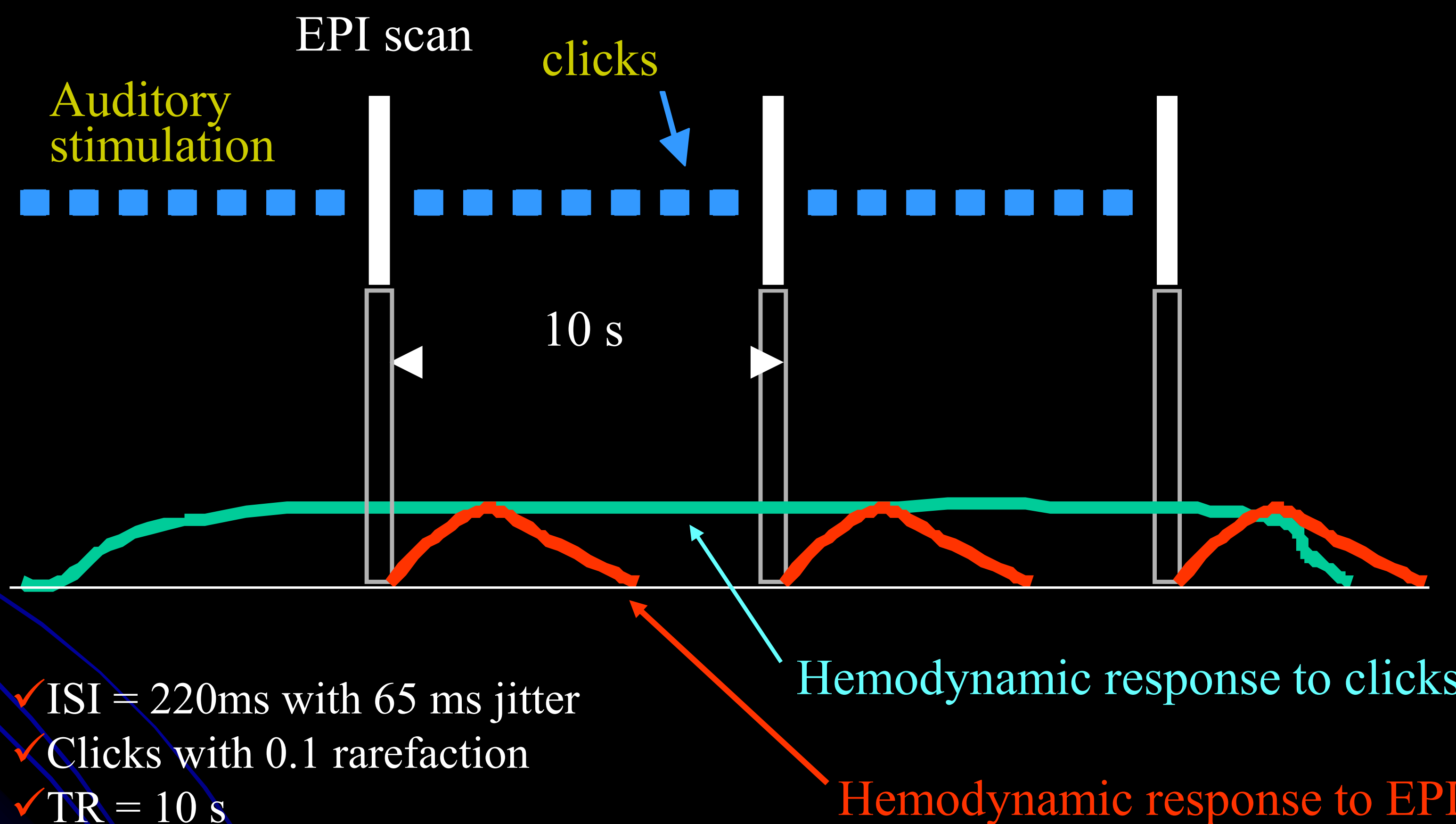

- ✓ISI = 220ms with 65 ms jitter
- ✓Clicks with 0.1 rarefaction
- ✓TR = 10 s
- ✓30s/30s ON/OFF (block paradigm)
- ✓180 fMRI time points (30 minutes scans)
- ✓1,000 averages per condition

AEPS 0÷3s after EPI (RED) and 3÷6s after EPI (BLUE) 3 Tesla

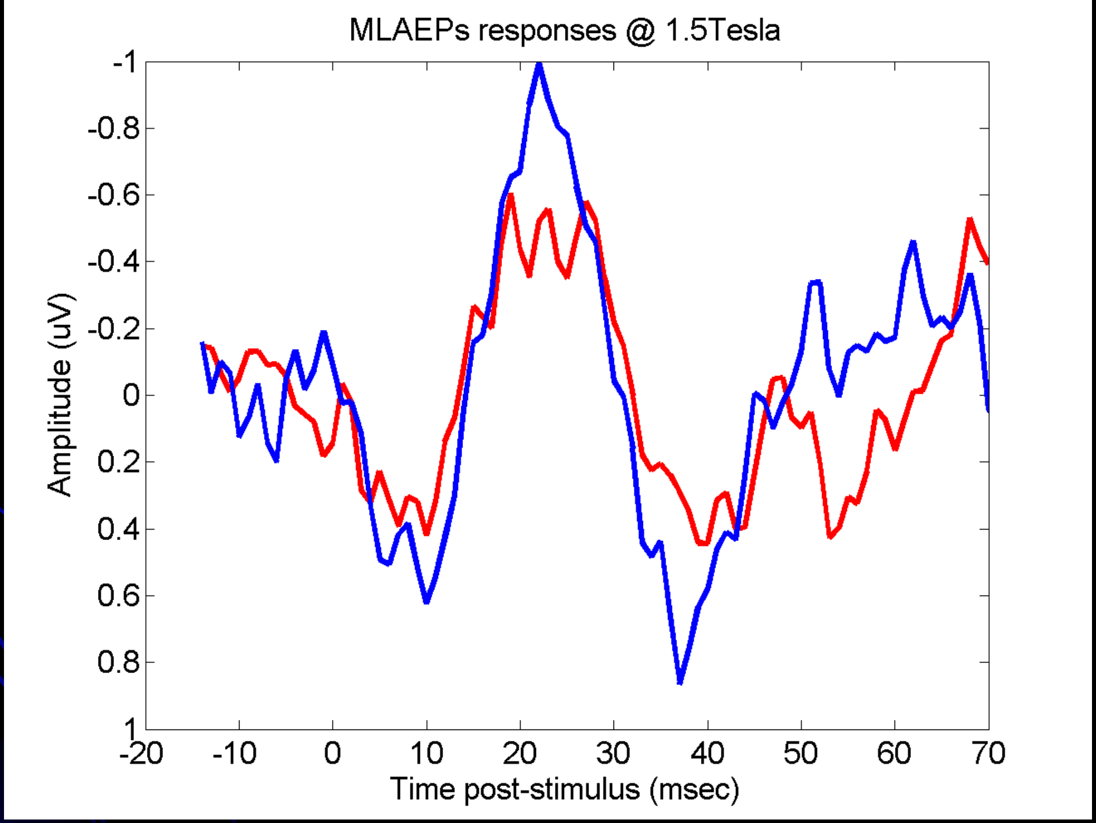

40 Hz Auditory Steady-State Response (ASSR)

- ERP from periodic click, tone, or noise-burst stimuli delivered at 40 Hz
- Compared to other frequencies, response greatest at 40 Hz (Galambos 1981)
- Abolished during loss of consciousness under general anesthesia (Plourde 1996, Meuret 2001)
- Gamma-band oscillations (~40 Hz) are related to binding and consciousness

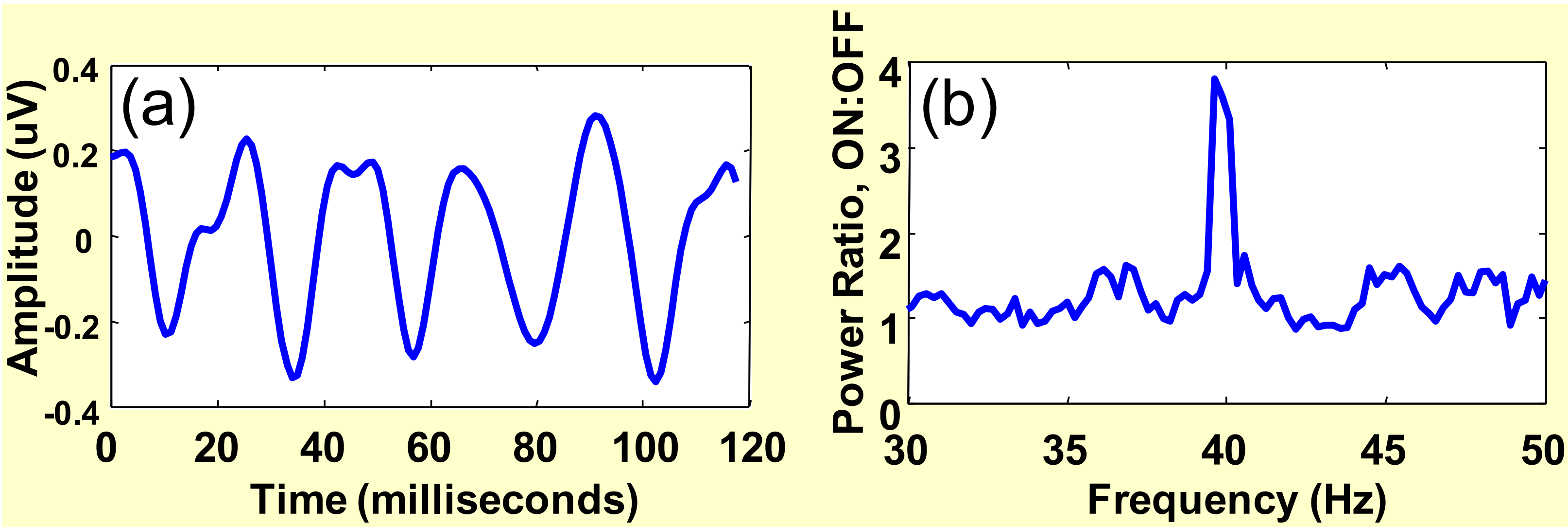

40-Hz ASSR in (a) time domain,(b) frequency domain

Concurrent Recording of 40-Hz Auditory Steady State Response (ASSR) and fMRI at 7T

- Noise bursts (40 Hz) of 30 sec followed by 30 sec break
- ASSRs are related to thalamo-cortical function and loss of consciousness.

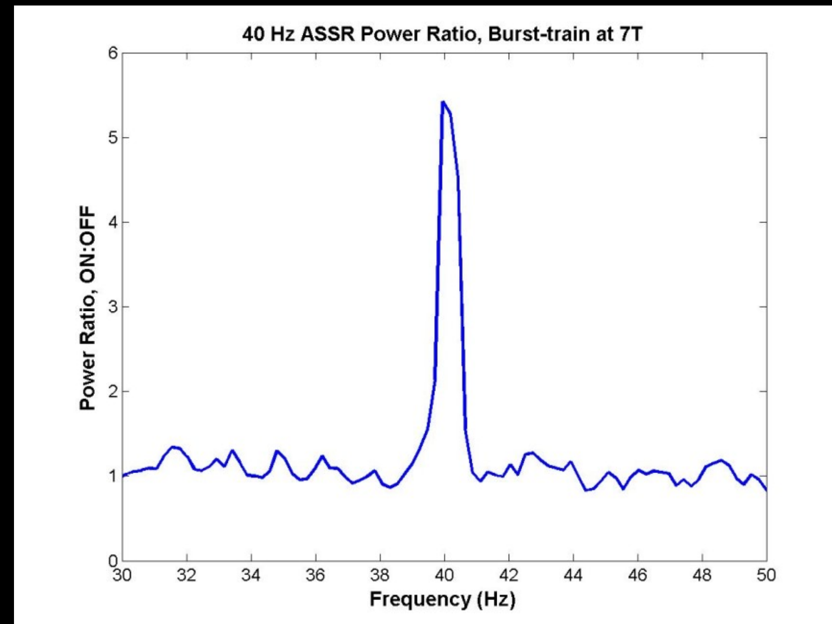

- BOLD activation map for 40Hz noise burst stimulus

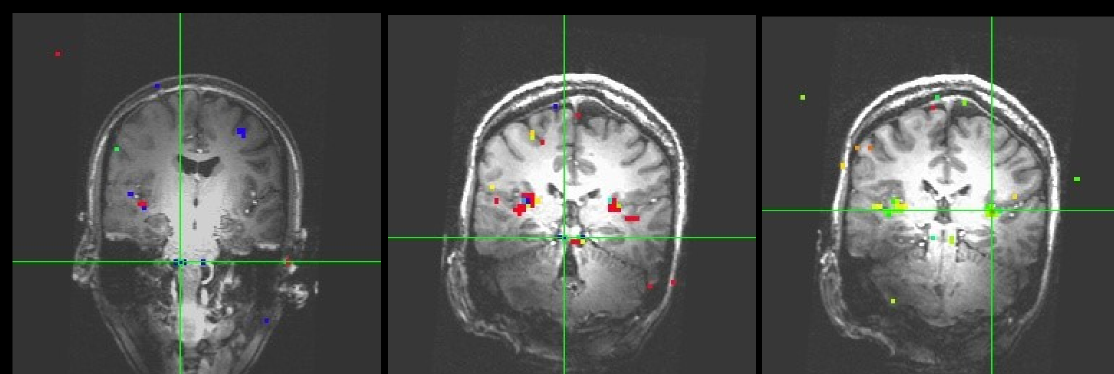

Results: Loss of Consciousness

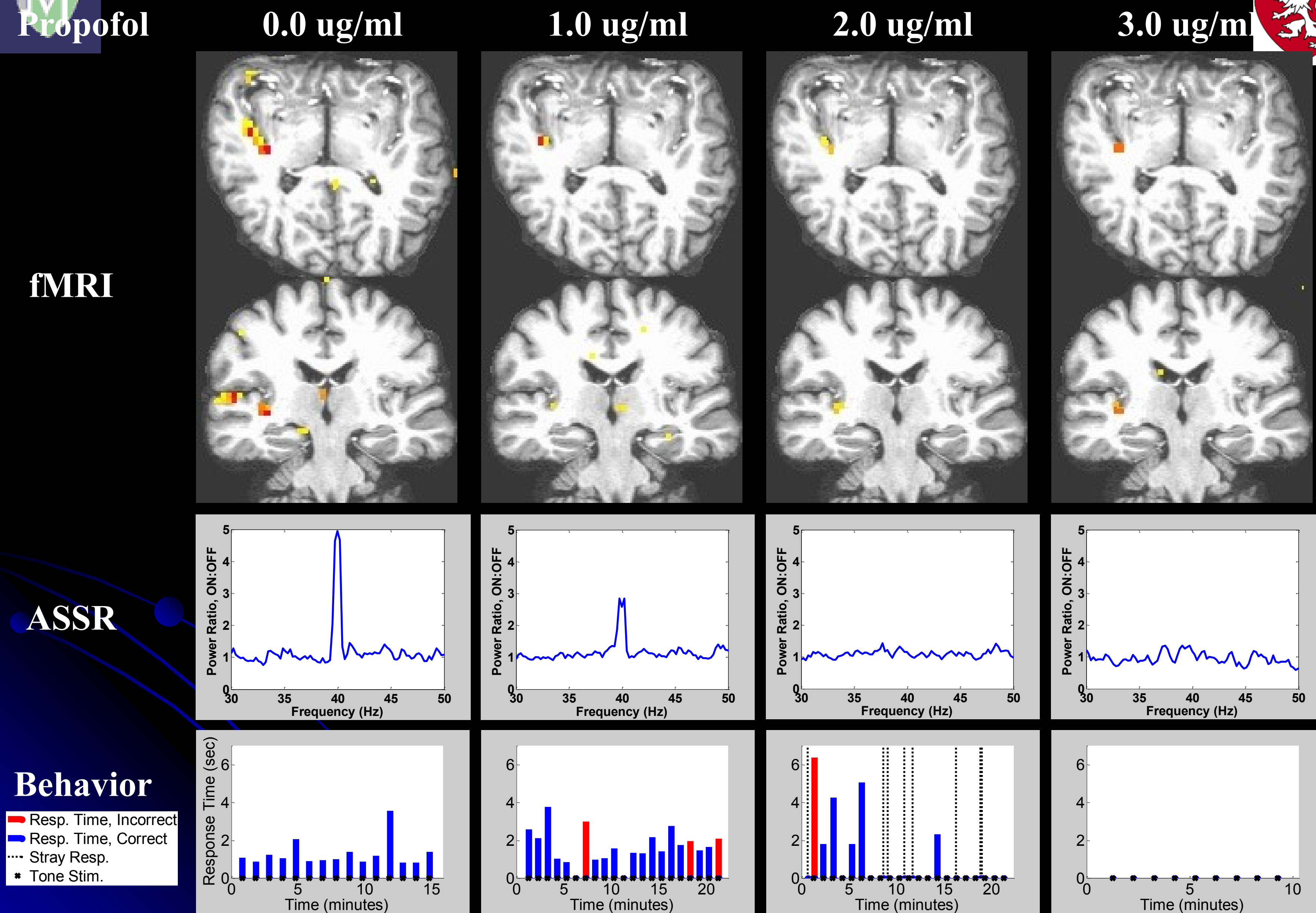

- Primary auditory cortex remains active after Loss of Consciousness (LOC)

Purdon et al. 2009 MGH

EEG/fMRI to study Sleep

Yotsumoto et al., 2009

Intensive training of TDT

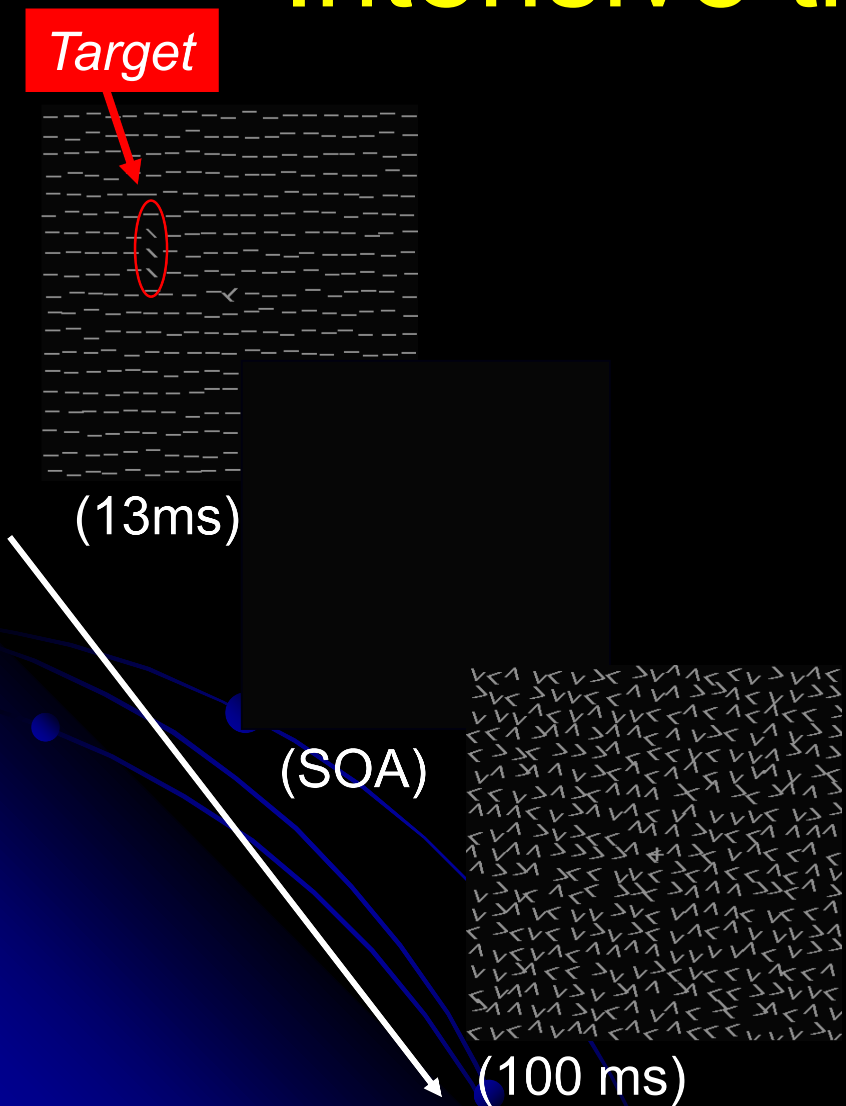

- Tasks (~90 min)
  - To report which of “T” or “L” is presented at the fixation
  - To report an orientation of the triplet
  - Always presented in a constant quadrant of the visual field
  - Trained visual field was counterbalanced across the subjects
- Stimulus-to-mask onset asynchrony (SOA) interval
  - The shorter SOA, the more difficult the orientation task
- To estimate subjects performance
  - Correct response ratio in a given SOA
  - A threshold SOA (80% correct discrimination)

Yotsumoto et al., 2009

Precise V1 localization

- Retinotopic mapping
  - To localize boundaries between V1, V2 (secondary visual area) etc.
    - Engel et al., 1994; Sereno 1995; Fize et al., 2003
  - Upper and lower visual fields
  - Eccentricity
- V1
  - Trained and untrained regions
  - If the trained visual field is the lower right visual field quadrant, then the corresponding trained V1 is the left dorsal part

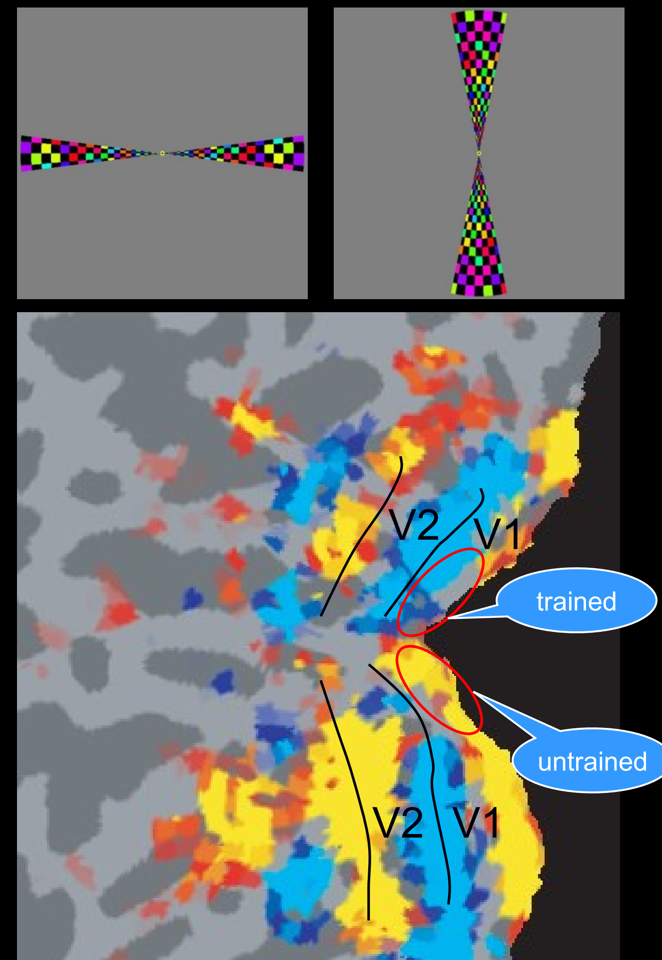

Left occipital cortex in a flattened format

Yotsumoto et al., 2009

PSG in 3T magnetic field Wakefulness

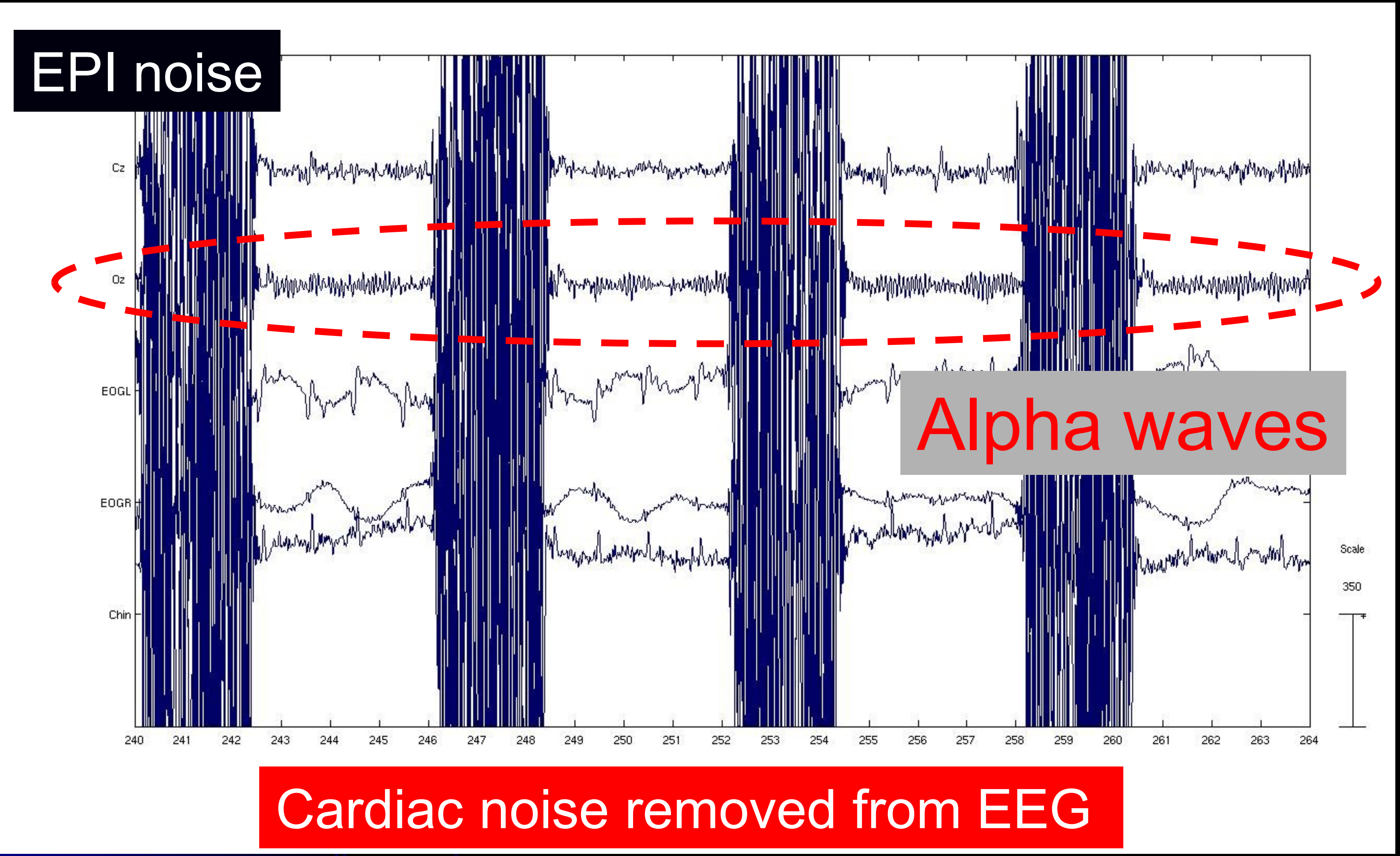

Yotsumoto et al., 2009

Sleep activity increased in the trained region during sleep periods

- Comparison of sleep activity
  - in the trained and untrained V1
  - in pre-training and post-training sleep sessions
- Subtraction of sleep activity in the untrained region from that in the trained regions (trained - untrained)
  - Nearly zero before training
  - The difference became larger after the training
  - BOLD signal increased in the trained region of V1

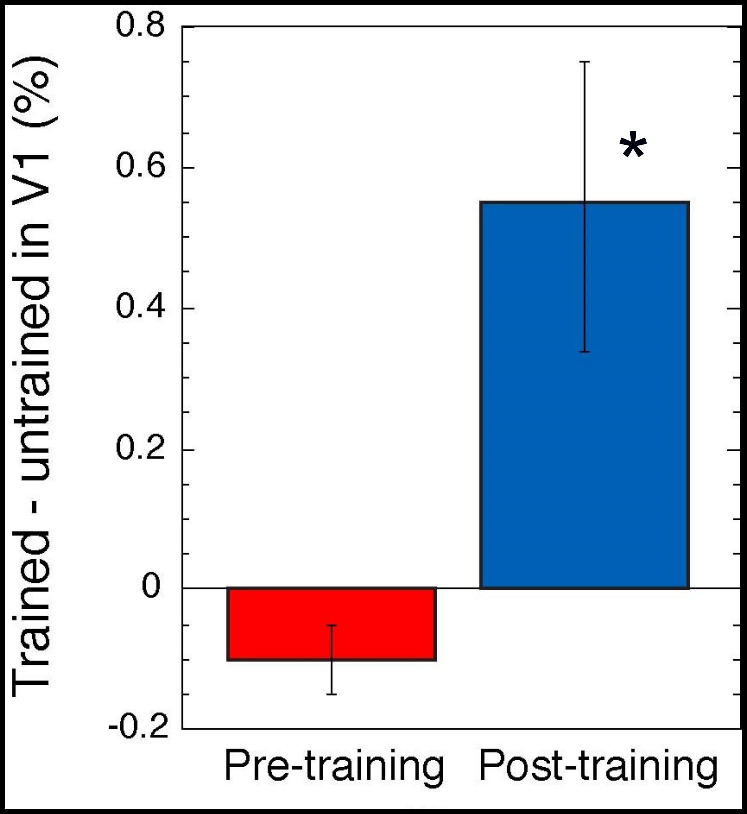

Yotsumoto et al., 2009

N=7

TDT performance was improved after the sleep period

- A threshold SOA (80%-SOA) was calculated in both the first training session and the re-test session
- In the re-test session, 80%-SOA became shorter by ~35 ms
- Performance was improved in the re-test

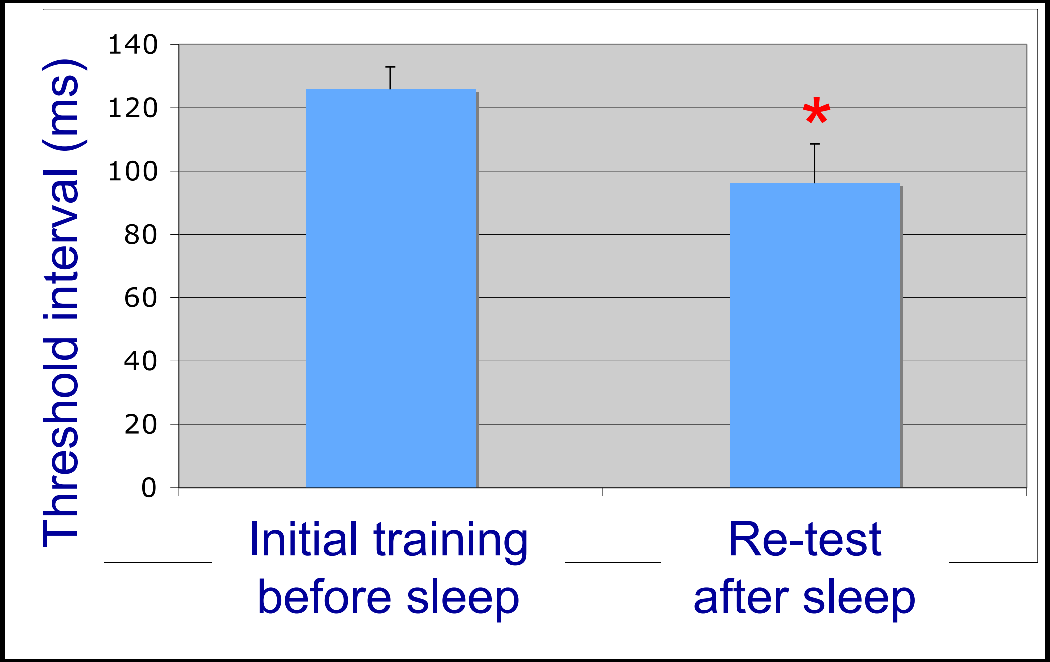

N=7

Resting State EEG/fMRI in Epilepsy

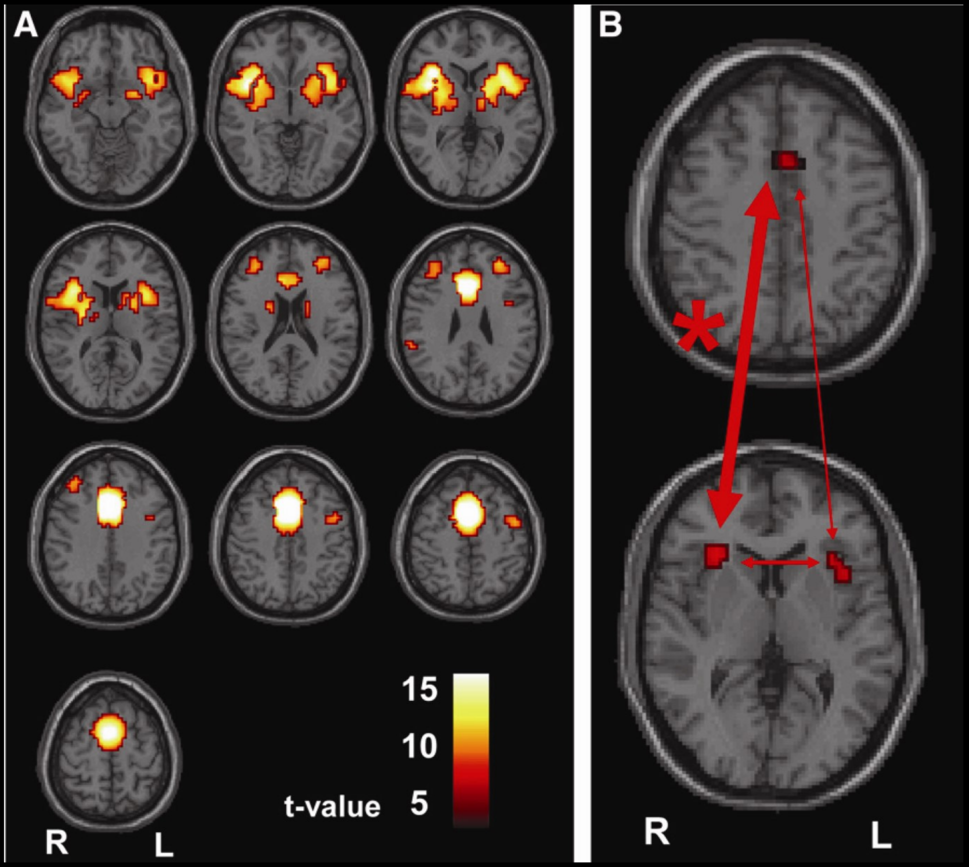

Resting functional connectivity analysis. A. Medial frontal ROI seed region shows maximal connectivity with bilateral anterior insula/frontal operculum, Mean z-score for connectivity between right In/FO

Killory, Impaired Attention…, Neuroimage 2011

Acknowledgements

MGH Martinos Center,
Charlestown, MA

Makris N. (CMA)
Purdon P.
Krishnaswamy P.
Angelone L.
Millan H.
Vasios C.
Brown E. (MIT)
Hamalainen M.
Fischl B.
Sasaki Y.
Yotsumono Y.
Ahveninen J.
Polimeni J.
Wald L.
Belliveau J.W.

Naval Submarine Medical Research
Center, US Navy

Michael, “Q” Chin.

Brigham and Women and BIDMC
Hospital, Boston, MA

Golby, A.
Schomer D.

Neurological Center
Tokyo, Japan

Anami, K.
Iwaki, S.

The University of Michigan

Solo, V.

University of KU Leuven (Belgium)

Van Duffel, W.